AIMS Mathematics, 11(4): 9398–9438.
DOI: 10.3934/math.2026390
Received: 18 January 2026
Revised: 18 March 2026
Accepted: 24 March 2026
Published: 08 April 2026

http://www.aimspress.com/journal/Math

Research article

Modeling and simulation of tax evasion dynamics: Optimal control and its cost-effectivenesss

Bharathi G S[1], Sagithya Thirumalai[1], Sekar Elango[2] and Bundit Unyong[3,*]

[1] School of Advanced Sciences, Vellore Institute of Technology, Chennai Campus, Chennai, 600127, Tamil Nadu, India

[2] Department of Mathematics, Amrita School of Physical Science, Coimbatore, Amrita Vishwa Vidyapeetham, India

[3] Department of Mathematics and Statistics, Center of Excellence for Ecoinformatics, School of Science, Walailak University, Nakhon Si Thammarat 80160, Thailand

* **Correspondence:** Email: bundit.un@wu.ac.th.

Abstract: Tax evasion remains a significant challenge that undermines government revenue and economic stability. In this paper, we propose proposes a new fractional-order three compartment tax evasion model that highlights the transition from susceptible individuals to honest taxpayers, capturing voluntary compliance driven by awareness and behavioral reinforcement mechanisms. The fundamental properties such as positivity, boundedness, and the existence and uniqueness of solutions, were established for the model. In this study, basic reproduction number (R_0) was derived to characterize the persistence of tax evasion. Stability analysis showed that the evader-free equilibrium was locally and globally asymptotically stable when the threshold parameter was less than one, and forward bifurcation occurred when the threshold parameter exceeded one, indicating the persistence of tax evasion. Sensitivity analysis using the Partial Rank Correlation Coefficient (PRCC) method identified that the influence rate (β) and the transition rate (α) are the dominant factors driving tax evasion, whereas audit effectiveness and reformation rate significantly reduce evasion. The model was numerically investigated using the Modified Fractional Euler Method (MFEM) for various combinations of parameters. Two control measures, namely media awareness campaigns (u_1) and penalties (u_2), are incorporated to mitigate tax evasion. Pareto and efficiency analyses revealed that penalties are effective when implemented individually, whereas the combined intervention strategy is the most cost-effective and economically viable approach for enhancing tax compliance. The results are presented in the form of figures and tables.

Keywords: tax evasion model; Caputo fractional derivative; PRCC; modified fractional Euler method; optimal control; cost effectiveness

Mathematics Subject Classification: 34A08, 49J15, 65L05

1. Introduction

Taxes are an important source for governments to generate revenue, which is used to fund critical public sector requirements such as education, healthcare, social services, pensions, infrastructure, and defense spending. Moreover, an efficient tax system is important for wealth redistribution, curbing harmful economic practices, curbing illegal financial flows, and fostering economic growth. Hence, it is important for a taxation system to be efficient, fair, and transparent. Public perceptions about the tax system play an important role in influencing the overall level of voluntary compliance and, in turn, the overall ability of the government to generate revenue.

Tax evasion is defined as the illegal concealment of income or financial information to reduce tax liability, which is considered one of the major challenges faced by taxation authorities globally. On the contrary, tax avoidance is defined as minimizing tax liability through legal means, adhering to tax regulation guidelines. Tax evasion is considered illegal, while tax avoidance is considered legal. In India, more than 8.09 crores of income tax returns filed during FY 2023-2024, only 6.68% of the total population filed tax returns [1]. Additionally, according to data reported till August 11, 2025, there was a decline of 1.87% in gross revenue and a decline of 3.95% in net collections in direct tax collections for FY 2025-26 [2]. In many situations, individuals who follow tax rules may face situations where factors such as the probability of getting caught while evading taxes may affect their decision to evade taxes.

In response to this challenge, governments around the world have enhanced enforcement strategies geared toward the fight against tax evasion, especially among high-income individuals and MNEs. One such strategy has been the monitoring of undeclared financial accounts and financial transactions [3,4]. This has been geared toward ensuring that fairness is enhanced in the tax system and that everyone is able to contribute as required. The importance of the underlying mechanisms of tax evasion is vital in the development of effective policies geared toward promoting compliance.

Tax evasion has been extensively analyzed in various studies, theoretically, empirically, and computationally. Economic models developed to understand tax evasion in earlier times suggest that tax evasion is a rational act in which taxpayers weigh the potential benefits of tax evasion against the potential costs of being audited by tax authorities. Later studies have also shown that social factors such as taxpayers' trust in government institutions affect their willingness to comply with tax laws [5]. Dynamic macroeconomic models have also shown that tax evasion can affect capital formation in an economy, thereby affecting productivity, particularly in those economies where taxpayers have heterogeneous opportunities to evade taxes [6]. Empirical studies have also shown that tax auditing can help reduce tax avoidance to a certain extent; however, this depends on taxpayers' behavior in the long run [7].

Zheng et al. [8] presented a comprehensive survey on tax risk detection methods using data mining and artificial intelligence techniques in 2024. They reviewed global research on tax risk detection, divided tax risk detection methods into relationship-based and non-relationship-based methods, and analyzed various tax risk detection algorithms, such as machine learning, clustering and neural

networks. Tax risk detection methods, such as tax evasion and tax fraud were discussed, as well as the challenges faced, such as tax data fragmentation and high cost of using algorithms. Knowledge-guided big data and intelligent tax have been shown as future trends in tax risk detection. In a study by Gombár, Svetozarovová, and Tóth in 2026 [9], a model for tax evasion was proposed based on a predator-prey model from the Lotka-Volterra system. In this study, tax evasion and enforcement were modeled as a nonlinear dynamic system with feedback loops. Their study demonstrates that fiscal systems may have a stable equilibrium, periodic oscillations, or instability depending on the efficiency and capacity of enforcement and institutional frameworks. The model demonstrates that adaptive regulation is required for long-run fiscal stability and tax compliance.

In the context of the diffusion of tax evasion in the population, mathematical models based on the structure of epidemiological models [10, 11] have also been proposed. In these mathematical models, the population is divided into compartments, including honest taxpayers, susceptible individuals, and active evaders. The transition between the compartments is driven by social interactions. In this context, Brum and Crokidakis [12] proposed a mathematical model in 2017, in which the population of taxpayers was divided into three groups: honest taxpayers, evaders, and susceptible individuals. The proposed mathematical model analysis was performed on different network structures, including a fully connected network, a scale-free network, and a random network. The analysis of the proposed mathematical model indicated that the spread of tax evasion is driven by social interactions. After the development of the classical mathematical model, it is essential to consider the limitations of the integer-order system in the accurate description of behavioral dynamics. For instance, in a number of socio-economic scenarios, such as tax evasion, the decisions made by an individual are not based solely on the current situation but are also influenced by past events such as audits and penalties. In this case, fractional calculus [13–15] is considered an appropriate tool for the system to remember the hereditary properties.

In 2021, a fractional order economic growth model with time delay was proposed by Lin and Wang [16] based on the classical Solow economic growth model. This model was motivated by the memory effects of economic growth. The results showed that fractional order derivatives can better describe the economic growth with memory effects. Furthermore, the memory effects of economic growth can be better described by fractional order derivatives. For example, Johansyah et al. [17] presented a comprehensive overview of fractional differential equations in economic growth models in 2021. The results showed that economic growth is a memory phenomenon, and fractional order derivatives can better describe it. For example, in 2025, Sylvia and Ghosh [18] analyzed a fractional order model of tax evasion in Caputo sense and solved it by an efficient numerical method, known as the Genocchi Wavelet Method (GWM).

Despite these advancements, most of the models of tax evasion, including earlier models, do not account for certain realistic behavioral transitions. For instance, most models do not account for the direct transition from susceptible individuals to honest taxpayers, which limits their ability to fully account for the dynamics of compliant behavior as a result of social influence and individual decision-making processes. To overcome this limitation, we propose a model for tax evasion based on a fractional order and use the Caputo derivative. In this model, the transition from susceptible individuals to honest individuals is included, which represents the possibility that dissatisfied individuals may return to honest behavior due to increased awareness and enforcement measures or due to influences from others. The proposed model based on the Caputo derivative is advantageous as it considers

memory effects and classical initial conditions.

The key highlights of the paper are summarized as follows:

- A novel model is developed by incorporating the transition from susceptible individuals to honest taxpayers, thereby capturing voluntary compliance behavior.
- The fundamental mathematical properties, including positivity, boundedness, and the existence and uniqueness of solutions, are established for the proposed model.
- The equilibrium points of the model are derived, and their stability, along with the bifurcation behavior of the system, are analyzed.
- Sensitivity analysis using the Partial Rank Correlation Coefficient (PRCC) method is performed to identify the most influential parameters governing the dynamics of tax evasion.
- Numerical simulations using the Modified Fractional Euler Method are performed to analyze the dynamic behavior of the system.
- An optimal control framework is developed by incorporating two scenarios with three strategies, and the effectiveness of these strategies is assessed through Pareto efficiency and cost-effectiveness analysis.

The study is organized as follows: Preliminary results are discussed in Section 2. In Section 3, we outline the model formulation. The positivity and boundedness of the system followed by the existence and uniqueness of solutions are studied in Section 4. The stability analysis is discussed in Section 5, and a detailed bifurcation analysis is conducted in Section 6. Sensitivity analysis is carried out in Section 7. In Section 8, numerical simulations are performed using the Modified Fractional Euler Method. In Section 9, we address the optimal control problem along with pareto, efficiency, and cost-effectiveness analysis. The major findings and conclusions are summarized in Section 10.

2. Preliminary results

In this section, we present some fundamental concepts and results from fractional calculus that will be useful in the subsequent analysis.

Definition 2.1. The Caputo fractional derivative of order $\rho > 0$ for a function $f(t)$ is defined as

$$ {}^{C}D_t^{\rho} f(t) = \frac{1}{\Gamma(n-\rho)} \int_0^t (t-s)^{n-\rho-1} f^{(n)}(s)\, ds, \tag{2.1} $$

where $n = \lceil \rho \rceil$ is the smallest integer, not less than ρ, and $f^{(n)}(s)$ denotes the classical n-th derivative of f.

Definition 2.2. The Laplace transform of the Caputo derivative of order ρ for a function $f(t)$, with $n = \lceil \rho \rceil$, is given by

$$ \mathcal{L}\left[{}^{C}D_t^{\rho} f(t) \right] = s^{\rho} F(s) - \sum_{k=0}^{n-1} s^{\rho-k-1} f^{(k)}(0), $$

where $F(s) = \mathcal{L}[f(t)]$ represents the Laplace transform of $f(t)$.

Definition 2.3. The two-parameter Mittag–Leffler function with $\rho > 0$ and $\beta > 0$ is defined as

$$E_{\rho,\beta}(z) = \sum_{k=0}^{\infty} \frac{z^k}{\Gamma(\rho k + \beta)}.$$

In particular, for $\beta = 1$, one recovers the standard Mittag–Leffler function $E_\rho(z)$. Its Laplace transform satisfies

$$\mathcal{L}[E_\rho(\mp\gamma t^\rho)] = \frac{s^{\rho-1}}{s(s^\rho \pm \gamma)}, \quad \mathcal{L}[1 - E_\rho(\mp\gamma t^\rho)] = \frac{\pm\gamma}{s(s^\rho \pm \gamma)}.$$

Lemma 2.1. *Consider the fractional differential equation*

$$D_t^\rho f(t) = g(t), \quad t \in [0, T],$$

with initial condition $f(0) = f_0$. Then, the solution can be written in the integral form

$$f(t) = f_0 + \frac{1}{\Gamma(\rho)} \int_0^t (t - s)^{\rho-1} g(s)\, ds.$$

Lemma 2.2. *[22] Let $f(t) \in C([0, T])$ with ${}^C D_t^\rho f(t) \in C(0, T]$ for some $\rho \in (0, 1]$. Then, for every $t \in (0, T]$, there exists $\iota \in [0, t]$ such that*

$$f(t) = f(0) + \frac{t^\rho}{\Gamma(\rho + 1)} {}^C D_t^\rho f(\iota). \tag{2.2}$$

Remark 2.1. *From Lemma 2.2, the following properties hold:*

1. *If ${}^C D_t^\rho f(t) \geq 0$, then $f(t)$ is non-decreasing on $(0, T]$.*
2. *If ${}^C D_t^\rho f(t) \leq 0$, then $f(t)$ is non-increasing on $(0, T]$.*

3. Model formulation

In this section, based on the literature, a new fractional-order tax evasion model is proposed. The model comprises three compartments as follows:

- **Honest Taxpayers (H):** The individuals fully committed to paying taxes, including individuals who previously evaded but returned to compliance due to enforcement measures or social influence.
- **Susceptibles (S):** Dissatisfied taxpayers who currently comply but may choose to evade if they perceive greater benefits than risks.
- **Tax Evaders (E):** Individuals who deliberately avoid paying taxes, influenced by social interactions and the strength of enforcement.

The honest taxpayer group ($H(t)$) increases through recruitment at rate Λ and through individuals returning from the susceptible and evader classes at rates δ, γ, and $q\eta$. It decreases when taxpayers become susceptible due to interaction with evaders at rate β and through natural exit at rate d. Thus,

$$\frac{dH(t)}{dt} = \Lambda - \beta \frac{H(t)E(t)}{N(t)} + \delta S(t) + \gamma E(t) + q\eta E(t) - dH(t). \tag{3.1}$$

The susceptible group ($S(t)$) rises through influence rate β. Individuals in this group may either enter evasion at rate α or return to honest tax payers group at rate δ, while natural removal occurs at rate d. Hence,

$$\frac{dS(t)}{dt} = \beta\frac{H(t)E(t)}{N(t)} - (\alpha + \delta + d)S(t). \tag{3.2}$$

The evader group ($E(t)$) grows as susceptible individuals adopt evasion at rate α. It declines when evaders reform at rate γ or when they are audited, with a detected fraction q successfully reinstated at rate η. Natural exit also contributes to reduction at rate d. Therefore,

$$\frac{dE(t)}{dt} = \alpha S(t) - (\gamma + q\eta + d)E(t). \tag{3.3}$$

In addition to the reform mechanism from evaders to honest taxpayers, the model also includes the transition from the susceptible class to the honest taxpayer class. The susceptible class includes people who are in the honest taxpayer class but may be uncertain about their position. However, they may also strengthen their commitment to becoming honest taxpayers through their own awareness, trust in government policies, and the community's support for the payment of taxes. This transition is a preventive mechanism that reduces the population of people who may transition to the evaders class. This transition is different from the reform mechanism from the evaders to the honest taxpayers class, where people return to becoming honest taxpayers because of audits and penalties.

Classical integer-order differential equations such as (3.1)–(3.3) assume that the evolution of each class depends only on its instantaneous rate of change. However, real-world taxpayer behavior frequently reflects memory effects and history-dependent decision patterns influenced by prior audits, policies, societal norms, and economic pressures. To capture these hereditary and nonlocal behaviors, the system is generalized to a fractional-order formulation using the Caputo derivative of order $0 < \rho \leq 1$.

Accordingly, the fractional tax evasion system becomes

$$\begin{aligned}
{}^{C}D_t^{\rho}H(t) &= \Lambda - \beta\frac{H(t)E(t)}{N(t)} + \delta S(t) + \gamma E(t) + q\eta E(t) - dH(t),\\
{}^{C}D_t^{\rho}S(t) &= \beta\frac{H(t)E(t)}{N(t)} - (\alpha + \delta + d)S(t),\\
{}^{C}D_t^{\rho}E(t) &= \alpha S(t) - (\gamma + q\eta + d)E(t),
\end{aligned} \tag{3.4}$$

with initial conditions $H(0) = a_1, \quad S(0) = a_2,$ and $\quad E(0) = a_3$, where $a_1, a_2, a_3 \geq 0$. ${}^{C}D_t^{\rho}$ denotes the Caputo derivative of order ρ. The schematic flow between compartments is illustrated in Figure 1.

The parameter values used in the numerical simulations are selected as representative baseline values within the parameter ranges considered in the PRCC–LHS global sensitivity analysis presented in Section 7. The parameter is defined, and the baseline values are summarized in Table 1.

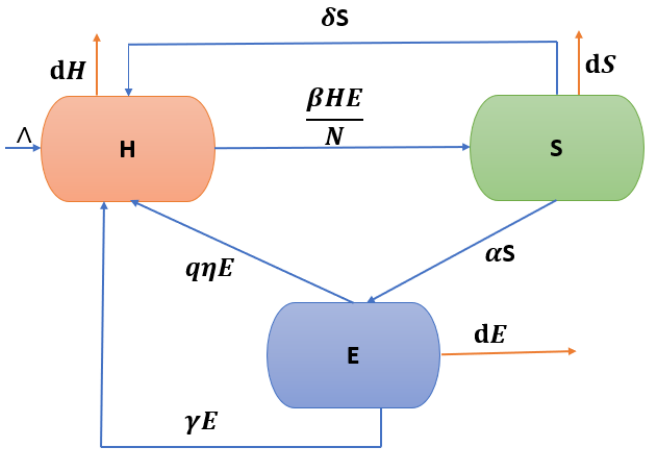

Figure 1. Diagrammatic representation of the model.

Table 1. Description of model parameters.

Parameter	Description	Value (day^{-1})
Λ	Recruitment rate (inflow of new taxpayers)	0.1
β	Influence rate of evaders on honest taxpayers	0.6
α	Rate at which susceptibles become evaders	0.2
δ	Rate at which susceptibles become honest tax payers	0.1
γ	Natural reformation rate	0.1
q	Proportion of evaders subject to audits	0.1
η	Audit success probability rate	0.2
d	Natural exit rate	0.001
N	Total population	800

4. Mathematical analysis

4.1. Positivity and boundedness of the system

The positivity of the solution is established in this section, as it is essential to demonstrate that the vector field points into $\mathbb{R}^3_+$ on each hyperplane bounding the positive orthant.

From the fractional model (3.4), we obtain:

$$
\begin{aligned}
{}^{C}D_t^{\rho} H(t)\Big|_{H=0} &= \Lambda + \delta S + \gamma E + q\eta E > 0,\\
{}^{C}D_t^{\rho} S(t)\Big|_{S=0} &= \frac{\beta HE}{N} > 0,\\
{}^{C}D_t^{\rho} E(t)\Big|_{E=0} &= \alpha S > 0.
\end{aligned}
$$

Hence, by utilizing Remark 2.1, it is verified that the solution remains confined within the positive orthant $\mathbb{R}^3_+$ for all $t \geq 0$.

Now, we proceed to demonstrate the boundedness of the system. Let $N(t) = H(t) + S(t) + E(t)$

represent the total population of tax payers. The rate of change of $N(t)$ is given by:

$$\begin{aligned} {}^{C}D_t^{\rho}N(t) &= {}^{C}D_t^{\rho}H(t) + {}^{C}D_t^{\rho}S(t) + {}^{C}D_t^{\rho}E(t) \\ &= \Lambda - d(H(t) + S(t) + E(t)) \\ &= \Lambda - dN(t). \end{aligned}$$

Taking the Laplace transform on both sides:

$$\begin{aligned} \mathcal{L}\left[{}^{C}D_t^{\rho}N(t)\right] + \mathcal{L}[dN(t)] &= \mathcal{L}[\Lambda], \\ s^{\rho}\mathcal{L}[N(t)] - s^{\rho-1}N(0) + d\mathcal{L}[N(t)] &= \frac{\Lambda}{s}, \\ \mathcal{L}[N(t)](s^{\rho} + d) &= \frac{\Lambda}{s} + s^{\rho-1}N(0), \\ \mathcal{L}[N(t)] &= \frac{\Lambda}{s(s^{\rho} + d)} + \frac{s^{\rho-1}N(0)}{s^{\rho} + d}. \end{aligned}$$

Taking the inverse Laplace transform, we get:

$$\begin{aligned} N(t) &= \frac{\Lambda}{d}\left(1 - E_{\rho}(-dt^{\rho})\right) + N(0)E_{\rho}(-dt^{\rho}), \\ N(t) &\leq \frac{\Lambda}{d}. \end{aligned}$$

Thus, the total population does not exceed $\frac{\Lambda}{d}$ as $t \to \infty$. Therefore, the biologically meaningful domain for the system is the following positively invariant region:

$$\Omega = \left\{(H, S, E) \in \mathbb{R}_+^3 : 0 \leq H + S + E \leq \frac{\Lambda}{d}\right\}.$$

4.2. Existence and uniqueness

In this section, we aim to prove the existence and uniqueness of solutions for the proposed fractional-order model. To begin, we define the set:

$$\Omega = \left\{(H, S, E) \in \mathbb{R}_+^3 : 0 \leq H + S + E \leq \frac{\Lambda}{d}\right\}.$$

The fractional differential equations (3.4), along with the initial condition, are rewritten in a more simplified form as follows:

$$\begin{aligned} {}^{C}D_t^{\rho}Z(t) &= F(t, Z(t)), \quad 0 < t < T < \infty \\ Z(0) &= Z_0 \end{aligned} \tag{4.1}$$

where $Z(t) = (H(t), S(t), E(t))^T$ and

$$F(t, Z(t)) = \begin{bmatrix} \Lambda - \dfrac{\beta HE}{N} + \delta S + \gamma E + q\eta E - dH \\ \dfrac{\beta HE}{N} - (\alpha + \delta)S - dS \\ \alpha S - \gamma E - q\eta E - dE \end{bmatrix} \tag{4.2}$$

with the initial condition $Z(0) = (H(0), S(0), E(0))^T$. Now, using Lemma 2.1 and (3.4), we obtain

$$Z(t) = Z(0) + \frac{1}{\Gamma(\rho)} \int_0^t (t-s)^{\rho-1} F(s, Z(s))\, ds. \tag{4.3}$$

Lemma 4.1. *The function $F(t, Z(t))$ specified in* (4.2) *satisfies the Lipschitz condition:*

$$\|F(t, Z_1(t)) - F(t, Z_2(t))\| \leq L\|Z_1 - Z_2\|, \tag{4.4}$$

where $L = \max\{L_1, L_2, L_3\}$, and $\|\cdot\|$ corresponds to the space $C([0,T], \mathbb{R}^3)$.

Proof. Let $Z = (H, S, E)$ and $\overline{Z} = (\overline{H}, \overline{S}, \overline{E})$.

$$\|F_1(t,Z) - F_1(t,\overline{Z})\| = \left\| \left(\Lambda - \frac{\beta HE}{N} + \delta S + \gamma E + q\eta E - dH \right) - \left(\Lambda - \frac{\beta \overline{H} E}{N} + \delta S + \gamma E + q\eta E - d\overline{H} \right) \right\|$$

$$\|F_1(t,Z) - F_1(t,\overline{Z})\| \leq L_1\|H - \overline{H}\| \text{ where, } L_1 = d + \frac{\beta C_1}{N} \text{ and } \|E\| < C_1.$$

$$\|F_2(t,Z) - F_2(t,\overline{Z})\| = \left\| \left(\frac{\beta HE}{N} - (\alpha + \delta)S - dS \right) - \left(\frac{\beta HE}{N} - (\alpha + \delta)\overline{S} - d\overline{S} \right) \right\|$$

$$\|F_2(t,Z) - F_2(t,\overline{Z})\| \leq L_2\|Z - \overline{Z}\| \text{ where } L_2 = \alpha + \delta + d.$$

$$\|F_3(t,Z) - F_3(t,\overline{Z})\| = \|\alpha S - \gamma E - q\eta E - dE - (\alpha S - \gamma \overline{E} - q\eta \overline{E} - d\overline{E})\|$$

$$\|F_3(t,Z) - F_3(t,\overline{Z})\| \leq L_3\|Z - \overline{Z}\| \text{ where } L_3 = \gamma + q\eta + d.$$

Thus,

$$\|F(t,Z) - F(t,\overline{Z})\| \leq L\|Z - \overline{Z}\|,$$

where $L = \max\{L_1, L_2, L_3\}$. Therefore, $F(t, Z(t))$ satisfies the Lipschitz condition with constant L. □

Lemma 4.2. *If the inequality $\frac{L}{\rho\Gamma(\rho)} T^\rho < 1$ is satisfied, then under the assumptions stated in* (4.4)*, the system* (3.4) *possesses a unique solution.*

Proof. Consider the fractional system (3.4), where the solution is defined by:

$$Z(t) = \mathbb{J}(Z(t)),$$

with the Picard operator $\mathbb{J}$ given by:

$$\mathbb{J}(Z(t)) = Z_0 + \frac{1}{\Gamma(\rho)} \int_0^t (t-s)^{\rho-1} F(s, Z(s))\, ds,$$

for $Z \in C([0,T], \mathbb{R}^3)$.

For the uniqueness, consider $Z_1, Z_2 \in C([0,T], \mathbb{R}^3)$. Then,

$$\begin{aligned} \|\mathbb{J}(Z_1(t)) - \mathbb{J}(Z_2(t))\| &= \left\| \frac{1}{\Gamma(\rho)} \int_0^t (t-s)^{\rho-1} \left(F(s, Z_1(s)) - F(s, Z_2(s)) \right) ds \right\| \\ &\leq \frac{1}{\Gamma(\rho)} \int_0^t (t-s)^{\rho-1} \|F(s, Z_1(s)) - F(s, Z_2(s))\| ds \end{aligned}$$

$$\leq \frac{L}{\Gamma(\rho)} \int_0^t (t-s)^{\rho-1} \|Z_1(s) - Z_2(s)\| ds.$$

Let $\|Z_1 - Z_2\| = \sup_{s\in[0,t]} \|Z_1(s) - Z_2(s)\|$. Then,

$$\begin{aligned} \|\mathbb{J}(Z_1(t)) - \mathbb{J}(Z_2(t))\| &\leq \frac{L}{\Gamma(\rho)} \|Z_1 - Z_2\| \int_0^t (t-s)^{\rho-1} ds \\ &= \frac{L}{\Gamma(\rho)} \|Z_1 - Z_2\| \cdot \frac{t^\rho}{\rho} \\ &\leq \frac{L}{\rho\Gamma(\rho)} T^\rho \|Z_1 - Z_2\|. \end{aligned}$$

Since, $\frac{L}{\rho\Gamma(\rho)} T^\rho < 1$, operator $\mathbb{J}$ is a contraction mapping on the Banach space $C([0,T], \mathbb{R}^3)$. Therefore, by the Banach fixed-point theorem, the fractional system (3.4) admits a unique solution.

□

5. Stability analysis of the model

5.1. Equilibrium points of the system

At equilibrium, we set ${}^C D_t^\rho H(t) = {}^C D_t^\rho S(t) = {}^C D_t^\rho E(t) = 0$, which leads to the algebraic system

$$\begin{aligned} \Lambda - \frac{\beta H E}{N} + \delta S + (\gamma + q\eta) E - d H &= 0, \\ \frac{\beta H E}{N} - (\alpha + \delta + d) S &= 0, \\ \alpha S - (\gamma + q\eta + d) E &= 0. \end{aligned}$$

5.1.1. Evaders-free equilibrium (EFE)

By setting $E = 0$, the system reduces to $\Lambda - dH = 0, S = 0$, which yields the evaders-free equilibrium

$$\boxed{M_0 = \left(\tfrac{\Lambda}{d},\ 0,\ 0\right)}.$$

5.1.2. Evaders-present equilibrium (EPE)

When $E > 0$, the system admits a positive equilibrium $M^* = (H^*, S^*, E^*)$, given by

$$H^* = \frac{\Lambda(\alpha + \delta + d)(\gamma + q\eta + d)}{\alpha d\beta}, \quad S^* = \frac{\Lambda(\gamma + q\eta + d)\left(\alpha\beta - (\alpha + \delta + d)(\gamma + q\eta + d)\right)}{\alpha d\beta(\alpha + \gamma + q\eta + d)},$$

$$E^* = \frac{\Lambda\left(\alpha\beta - (\alpha + \delta + d)(\gamma + q\eta + d)\right)}{d\beta(\alpha + \gamma + q\eta + d)}.$$

For biological feasibility ($H^*, S^*, E^* \geq 0$), the following condition is required:

$$\alpha\beta > (\alpha + \delta + d)(\gamma + q\eta + d).$$

This ensures $E^* > 0$ and $S^* > 0$, while H^* is always positive.

5.2. Basic reproduction number (R_0)

The basic reproduction number (R_0) represents the average number of new tax evaders generated by a single evader through social influence. If $R_0 < 1$, tax evasion gradually disappears, and the system approaches the evader-free equilibrium. If $R_0 > 1$, tax evasion can spread and persist in the population.

The rate of arrival of new evaders denoted by $\mathcal{F}$ and the transition matrix $\mathcal{V}$ is given by, is written as

$$\mathcal{F} = \begin{pmatrix} \frac{\beta HE}{N}, \\ 0 \end{pmatrix} \qquad \mathcal{V} = \begin{pmatrix} (\alpha + \delta + d)\, S \\ -\alpha S + (\gamma + q\eta + d)\, E \end{pmatrix}.$$

Let $k_1 = \alpha + \delta + d, k_2 = \gamma + q\eta + d$. The matrices $\mathcal{F}$ and $\mathcal{V}$ evaluated at M_0 are

$$\mathcal{F} = \begin{bmatrix} 0 & \frac{\beta H}{N} \\ 0 & 0 \end{bmatrix} = \begin{bmatrix} 0 & \beta \\ 0 & 0 \end{bmatrix}, \qquad \mathcal{V} = \begin{bmatrix} k_1 & 0 \\ -\alpha & k_2 \end{bmatrix}.$$

The inverse of $\mathcal{V}$ is

$$\mathcal{V}^{-1} = \frac{1}{k_1 k_2} \begin{bmatrix} k_2 & 0 \\ \alpha & k_1 \end{bmatrix} = \begin{bmatrix} \frac{1}{k_1} & 0 \\ \frac{\alpha}{k_1 k_2} & \frac{1}{k_2} \end{bmatrix}.$$

Thus, the next-generation matrix $K = \mathcal{F}\mathcal{V}^{-1}$ equals

$$K = \begin{bmatrix} 0 & \beta \\ 0 & 0 \end{bmatrix} \begin{bmatrix} \frac{1}{k_1} & 0 \\ \frac{\alpha}{k_1 k_2} & \frac{1}{k_2} \end{bmatrix} = \begin{bmatrix} \frac{\alpha\beta}{k_1 k_2} & \frac{\beta}{k_2} \\ 0 & 0 \end{bmatrix}.$$

The eigenvalues of K are 0 and $\frac{\alpha\beta}{k_1 k_2}$. Therefore, the basic reproduction number is

$$\boxed{R_0 = \frac{\alpha\beta}{(\alpha + \delta + d)\,(\gamma + q\eta + d)}}.$$

Figure 2 presents contour plots illustrating the influence of parameter combinations on the basic reproduction number (R_0). An increase in the susceptible-to-evader transition rate (α) leads to higher values of R_0, whereas a higher audit success rate (η), greater natural reformation rate (γ), and increased susceptible to honest transmission rate (δ) reduce R_0. Similarly, the influence rate of evaders on honest taxpayers (β) has a strong positive effect on R_0, reflecting the significant role of social influence in sustaining evasion. However, this effect is mitigated when γ, δ, or η increase. Notably, the combination of high α and high β produces the largest values of R_0, highlighting the reinforcing impact of susceptibility and peer influence. Overall, parameters that encourage evasion α, β substantially increase R_0, while those that promote honesty or strengthen enforcement γ, δ, q, η effectively suppress it. This interplay underscores the importance of enforcement mechanisms in shaping long-term tax compliance.

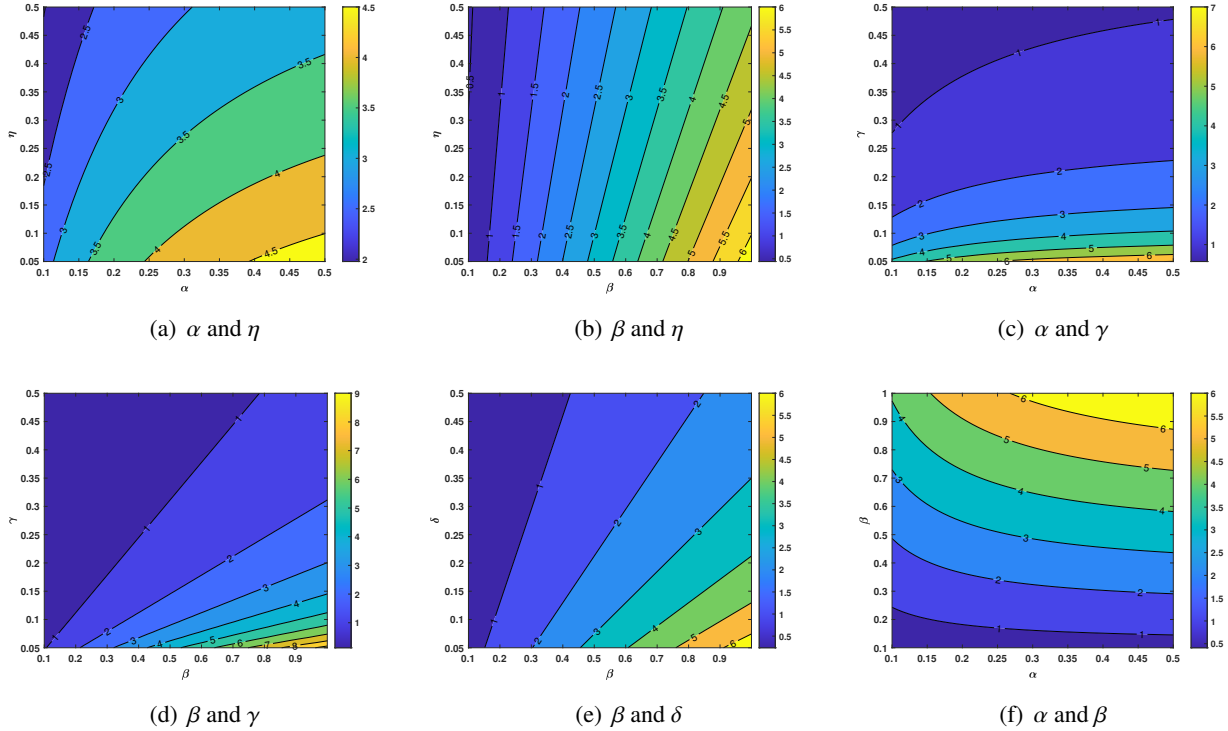

(a) α and η (b) β and η (c) α and γ

(d) β and γ (e) β and δ (f) α and β

Figure 2. Contour plots of the basic reproduction number (R_0) with respect to different parameter combinations.

5.3. Local and gobal stability

Theorem 5.1. *The evaders-free equilibrium (M_0) is locally asymptotically stable whenever $R_0 < 1$ and all eigenvalues λ_i, $i = 1, 2, 3$, of the Jacobian matrix evaluated at M_0 satisfy $\left|\arg(\lambda_i)\right| > \frac{\rho\pi}{2}$, where ρ denotes the fractional order of the system.*

Proof. The Jacobian matrix of system (3.4), evaluated at M_0, is

$$J(M_0) = \begin{bmatrix} -d & \delta & -\beta + \gamma + q\eta \\ 0 & -(\alpha + \delta + d) & \beta \\ 0 & \alpha & -(\gamma + q\eta + d) \end{bmatrix}. \tag{5.1}$$

One eigenvalue of $J(M_0)$ is $\lambda_1 = -d$. The other two eigenvalues are obtained from the quadratic characteristic equation

$$\begin{aligned} P(\lambda) &= \lambda^2 + [(\alpha + \delta + d) + (\gamma + q\eta + d)]\lambda + [(\alpha + \delta + d)(\gamma + q\eta + d) - \alpha\beta] = 0, \\ &= \lambda^2 + [(\alpha + \delta + d) + (\gamma + q\eta + d)]\lambda + (\alpha + \delta + d)(\gamma + q\eta + d)[1 - R_0] = 0. \end{aligned} \tag{5.2}$$

By applying the Routh–Hurwitz stability criterion, it follows that all roots of (5.2) have negative real parts. Consequently, their arguments satisfy the Matignon condition [19] $\left|\arg(\lambda_i)\right| > \frac{\rho\pi}{2}$, $i = 1, 2, 3$. Therefore, all eigenvalues of $J(M_0)$ satisfy the fractional-order stability condition, and hence the evaders-free equilibrium point M_0 is locally asymptotically stable for $R_0 < 1$. □

Theorem 5.2. *For the tax evasion model* (3.4)*, the evaders-free equilibrium* $M_0 = \left(\frac{\Lambda}{d}, 0, 0\right)$ *is globally asymptotically stable if* $\beta < \frac{(\alpha+\delta+d)(\gamma+q\eta+d)}{\alpha}$.

Proof. Consider the Lyapunov function:

$$\mathcal{V} = \left(H - H_0 - H_0 \ln \frac{H}{H_0}\right) + S + \frac{\alpha+\delta+d}{\alpha} E.$$

Applying the Caputo fractional derivative:

$$\begin{aligned}
{}^{C}D_t^{\rho}\mathcal{V} &= \left(1 - \frac{H_0}{H}\right){}^{C}D_t^{\rho}H + {}^{C}D_t^{\rho}S + \frac{\alpha+\delta+d}{\alpha}{}^{C}D_t^{\rho}E. \\
&= \left(1 - \frac{H_0}{H}\right)\left[\Lambda - \frac{\beta HE}{N} + \delta S + (\gamma+q\eta)E - dH\right] + \left[\frac{\beta HE}{N} - (\alpha+\delta+d)S\right] \\
&\quad + \frac{\alpha+\delta+d}{\alpha}\left[\alpha S - (\gamma+q\eta+d)E\right].
\end{aligned}$$

At the equilibrium M_0, $\Lambda = dH_0$.

$$\begin{aligned}
{}^{C}D_t^{\rho}\mathcal{V} &= \left(1 - \frac{H_0}{H}\right)(dH_0 - dH) + \left(1 - \frac{H_0}{H}\right)\left[-\frac{\beta HE}{N} + \delta S + (\gamma+q\eta)E\right] \\
&\quad + \frac{\beta HE}{N} - (\alpha+\delta+d)S + (\alpha+\delta+d)S - \frac{(\alpha+\delta+d)(\gamma+q\eta+d)}{\alpha}E. \\
{}^{C}D_t^{\rho}\mathcal{V} &= -d\frac{(H-H_0)^2}{H} - \frac{\beta HE}{N} + \frac{\beta HE}{N}\cdot\frac{H_0}{H} + \delta S\left(1 - \frac{H_0}{H}\right) + (\gamma+q\eta)E\left(1 - \frac{H_0}{H}\right) \\
&\quad + \frac{\beta HE}{N} - \frac{(\alpha+\delta+d)(\gamma+q\eta+d)}{\alpha}E. \\
&= -d\frac{(H-H_0)^2}{H} + \frac{\beta H_0 E}{N} + \frac{\delta S(H-H_0)}{H} + \frac{(\gamma+q\eta)E(H-H_0)}{H} - \frac{(\alpha+\delta+d)(\gamma+q\eta+d)}{\alpha}E. \\
{}^{C}D_t^{\rho}\mathcal{V} &= -d\frac{(H-H_0)^2}{H} + \frac{\delta S(H-H_0)}{H} + \frac{(\gamma+q\eta)E(H-H_0)}{H} + \beta E - \frac{(\alpha+\delta+d)(\gamma+q\eta+d)}{\alpha}E. \\
&= -d\frac{(H-H_0)^2}{H} + \frac{\delta S(H-H_0)}{H} + \frac{(\gamma+q\eta)E(H-H_0)}{H} + \left(\beta - \frac{(\alpha+\delta+d)(\gamma+q\eta+d)}{\alpha}\right)E.
\end{aligned}$$

If $R_0 < 1$, $R_0 = \frac{\alpha\beta}{(\alpha+\delta+d)(\gamma+q\eta+d)} < 1 \implies \alpha\beta < (\alpha+\delta+d)(\gamma+q\eta+d) \implies \beta < \frac{(\alpha+\delta+d)(\gamma+q\eta+d)}{\alpha}$. Therefore, ${}^{C}D_t^{\rho}\mathcal{V} \leq 0$ if $R_0 \leq 1$ and $H \leq H_0$. Moreover, ${}^{C}D_t^{\rho}\mathcal{V} = 0$ if and only if $H = H_0$ and $R_0 = 1$. Therefore, the evaders-free equilibrium M_0 is globally asymptotically stable when $R_0 < 1$. □

Theorem 5.3. *For the model* (3.4)*, the evaders-present equilibrium* (M^*) *is globally asymptotically stable if* $R_0 > 1$.

Proof. The Lyapunov function is defined as follows:

$$\mathcal{V} = (H - H^* \ln H) + (S - S^* \ln S) + (E - E^* \ln E). \tag{5.3}$$

$$\begin{aligned}
{}^{C}D_t^{\rho}\mathcal{W}(t) &= {}^{C}D_t^{\rho}\left[(H - H^* \ln H) + (S - S^* \ln S) + (E - E^* \ln E)\right] \\
&= \left(1 - \frac{H^*}{H}\right){}^{C}D_t^{\rho}H + \left(1 - \frac{S^*}{S}\right){}^{C}D_t^{\rho}S + \left(1 - \frac{E^*}{E}\right){}^{C}D_t^{\rho}E.
\end{aligned}$$

Substituting all the expressions for the fractional derivatives from Eq (3.4), we get:

$$
\begin{aligned}
{}^{C}D_t^{\rho}\mathcal{W}(t) &= \left(1-\frac{H^*}{H}\right)\left(\Lambda-\frac{\beta HE}{N}+\delta S+(\gamma+q\eta)E-dH\right)+\left(1-\frac{S^*}{S}\right)\left(\frac{\beta HE}{N}-(\alpha+\delta+d)S\right)\\
&\quad+\left(1-\frac{E^*}{E}\right)(\alpha S-(\gamma+q\eta+d)E)\,.\\
&=\Lambda-\frac{\beta HE}{N}+\delta S+(\gamma+q\eta)E-dH-\frac{\Lambda H^*}{H}+\frac{H^*}{H}\frac{\beta HE}{N}-\frac{\delta S H^*}{H}-\frac{(\gamma+q\eta)EH^*}{H}+dH^*-\frac{\alpha S E^*}{E}\\
&\quad+\frac{\beta HE}{N}-(\alpha+\delta+d)S-\frac{S^*}{S}\frac{\beta HE}{N}+(\alpha+\delta+d)S^*+\alpha S-(\gamma+q\eta+d)E+(\gamma+q\eta+d)E^*.
\end{aligned}
\tag{5.4}
$$

Here, (5.4) is rewritten as ${}^{C}D_t^{\nu}\mathcal{W}(t)=\Pi_1-\Pi_2$
where,

$$\Pi_1=\Lambda+dH^*+(\alpha+\delta+d)S^*+(\gamma+q\eta+d)E^*+\frac{H^*}{H}\frac{\beta HE}{N}.$$

$$\Pi_2=dH+\frac{\Lambda H^*}{H}+\frac{\delta S H^*}{H}+\frac{(\gamma+q\eta)EH^*}{H}+\frac{S^*}{S}\frac{\beta HE}{N}+\frac{E^*}{E}\alpha S.$$

As each parameter of model (3.4) is positive, we have ${}^{C}D_t^{\nu}\mathcal{W}(t)<0 \quad \text{if} \quad \Pi_1<\Pi_2$. The equality ${}^{C}D_t^{\nu}\mathcal{W}(t)=0$ holds if and only if $\Pi_1=\Pi_2$ □

6. Bifurcation analysis

In this section, we perform a bifurcation analysis to examine the qualitative behavior of the tax evasion model changes as the influence rate β approaches the threshold $R_0=1$. The center manifold theory is employed to reduce the system near the equilibrium point and to determine the type of bifurcation based on the signs of the bifurcation coefficients.

Let $x=[x_1,x_2,x_3]^T=[H,S,E]^T$. Then the model can be written compactly as

$$
\begin{aligned}
{}^{C}D_t^{\nu}x_1&=\Lambda-\frac{\beta x_1x_3}{N}+\delta x_2+(\gamma+q\eta)x_3-dx_1=f_1,\\
{}^{C}D_t^{\nu}x_2&=\frac{\beta x_1x_3}{N}-(\alpha+\delta+d)x_2=f_2,\\
{}^{C}D_t^{\nu}x_3&=\alpha x_2-(\gamma+q\eta+d)x_3=f_3.
\end{aligned}
\tag{6.1}
$$

Choosing β as the bifurcation parameter and setting $R_0=1$, we obtain

$$\beta=\beta^*=\frac{(\alpha+\delta+d)(\gamma+q\eta+d)}{\alpha}.\tag{6.2}$$

The Jacobian matrix evaluated at the evaders free equilibrium M_0 and $\beta=\beta^*$, denoted by $J(E_0,\beta^*)$, is given by

$$J(M_0,\beta^*)=\begin{bmatrix}-d & \delta & -\beta+\gamma+q\eta\\ 0 & -(\alpha+\delta+d) & \beta\\ 0 & \alpha & -(\gamma+q\eta+d)\end{bmatrix}.\tag{6.3}$$

It can be established using the Routh–Hurwitz criterion that $J(E_0, \beta^*)$ has a simple zero eigenvalue, while the remaining eigenvalues exhibit negative real parts. Let

$$w = [w_1, w_2, w_3]^T, \qquad v = [v_1, v_2, v_3]$$

represent the right and left eigenvectors corresponding to the zero eigenvalue respectively. Solving $J(E_0, \beta^*)w = 0$ and $vJ(E_0, \beta^*) = 0$, we obtain

$$w_1 = -\frac{\alpha + \gamma + q\eta + d}{\alpha}, \quad w_2 = \frac{\gamma + q\eta + d}{\alpha}, \quad w_3 = 1,$$

and

$$v_1 = 0, \quad v_2 = \frac{\alpha}{\alpha + \delta + d}, \quad v_3 = 1.$$

To determine the bifurcation type, we compute the coefficients as follows:

$$a = \sum_{k=1}^{3}\sum_{i=1}^{3}\sum_{j=1}^{3} v_k w_i w_j \frac{\partial^2 f_k}{\partial x_i \partial x_j}(M_0, \beta^*), \qquad b = \sum_{k=1}^{3}\sum_{i=1}^{3} v_k w_i \frac{\partial^2 f_k}{\partial x_i \partial \beta}(M_0, \beta^*). \tag{6.4}$$

Computing the second partial derivatives of $f_i (i = 1, 2, 3)$ and using the values in equations above, we obtain:

$$a = -\frac{(\alpha + \gamma + q\eta + d)(\gamma + q\eta + d)}{\alpha N} < 0, \qquad b = \frac{\alpha}{\alpha + \delta + d} > 0. \tag{6.5}$$

Since $a < 0$ and $b > 0$, the bifurcation that occurs at $\beta = \beta^*$ is a forward bifurcation.

Theorem 6.1. *The tax evasion model* (3.4) *undergoes a forward bifurcation at $\beta = \beta^*$ whenever the bifurcation coefficients satisfy $a < 0$ and $b > 0$.*

6.1. Bifurcation diagram

Figure 3 illustrates the qualitative behavior of the evader population E with respect to the influence transmission parameter β. When $\beta < \beta^*$, the basic reproduction number $R_0 < 1$, and the system settles at the evader–free equilibrium (EFE), represented by the blue branch indicating the absence of tax evaders in the population. This equilibrium remains locally asymptotically stable until the critical point $\beta = \beta^*$.

The smooth transition occurs when β is at the threshold value β^*, where the EFE loses stability, creating a stable evaders present equilibrium (EPE), represented by the red curve. As β increments above the value of β^*, the evaders steadily increase, validating the existence of a forward bifurcation. This means that if the rate of influence of evaders on honest taxpayers exceeds the critical threshold β^*, then tax evasion becomes self-sustaining in the society. However, policies aimed at reducing tax evasion by lowering β below the threshold β^* ensure that there is total eradication of tax evasion and the system returns to the stationary EFE.

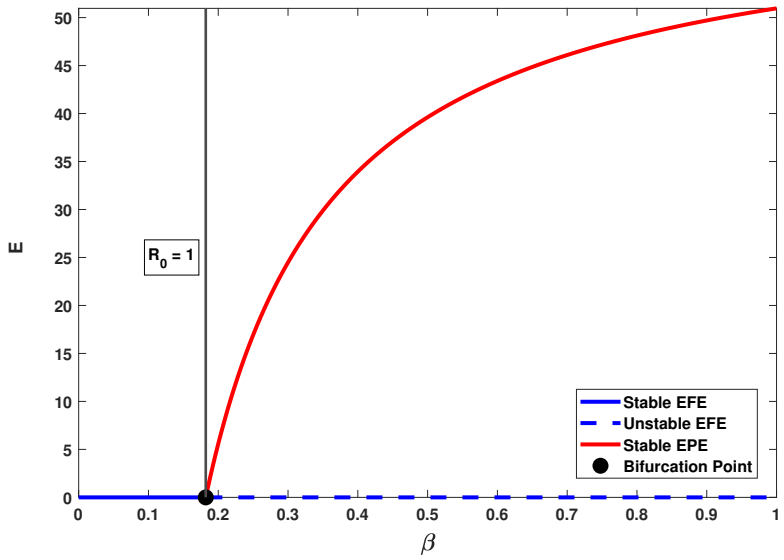

Figure 3. Bifurcation diagram at $R_0 = 1$.

7. Sensitivity analysis

7.1. Normal forward sensitivity index

Sensitivity analysis is conducted to assess the parameters that affect the basic reproduction number (R_0) of tax evasion. A parameter with a larger value of sensitivity index impacts the value of R_0 significantly, making this parameter more important in the determination of the persistence of tax evasion in society.

The normalized forward sensitivity index of a parameter ω with respect to R_0 is defined as

$$I_{\omega}^{R_0} = \frac{\partial R_0}{\partial \omega} \cdot \frac{\omega}{R_0}.$$

The sensitivity analysis, illustrated in Table 2 and Figure 4, indicates that the influence rate of evaders on honest taxpayers (β) holds the strongest positive impact on the basic reproduction number, with a sensitivity index of 1. This means that a 1% increase in β results in a direct 1% increase in R_0, demonstrating that even slight rises in evader influence substantially enhance the spread of tax evasion. The rate at which susceptibles become evaders (α) also contributes positively, where a 1% rise in α produces an approximate 0.34% increase in R_0. Together, these two parameters act as the major drivers of tax evasion.

Table 2. Sensitivity indices for R_0 in percentage interpretation.

α	β	δ	γ	q	η	d
0.3355	1.000	−0.3322	−0.8264	−0.1653	−0.1653	−0.0116

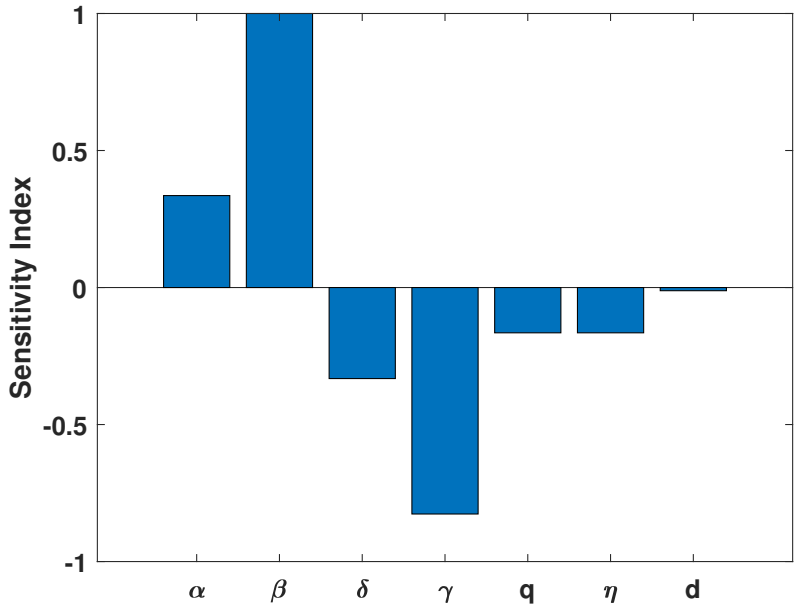

Figure 4. Sensitivity analysis of the tax evasion model.

In contrast, a rise of 1% in the natural rate of reformation (γ) reduces R_0 by approximately 0.83%, indicating a strong depressant effect. A corresponding escalation of the transition rate of the susceptible population to honest taxpayers (δ) by 1% generates a reduction of 0.33% in the value of R_0, while a rise of the same amount for the audit percentage (q) and success probability (η) generates a reduction of 0.17% for each variable. These findings suggest that strengthening reform pathways and increasing enforcement intensity reduce the persistence of tax evasion.

In addition, the natural exit rate (d) has a very small negative index, showing that its effect on tax evasion dynamics is negligible. The critical parameter values at which the transcritical bifurcation occurs are shown in Figure 5. From these observations, we conclude that control policies should primarily aim to reduce the influence of tax evaders and lower the rate at which susceptibles become tax evaders. Furthermore, measures that increase honest behavior through reformation and audits can help suppress the prevalence of tax evasion.

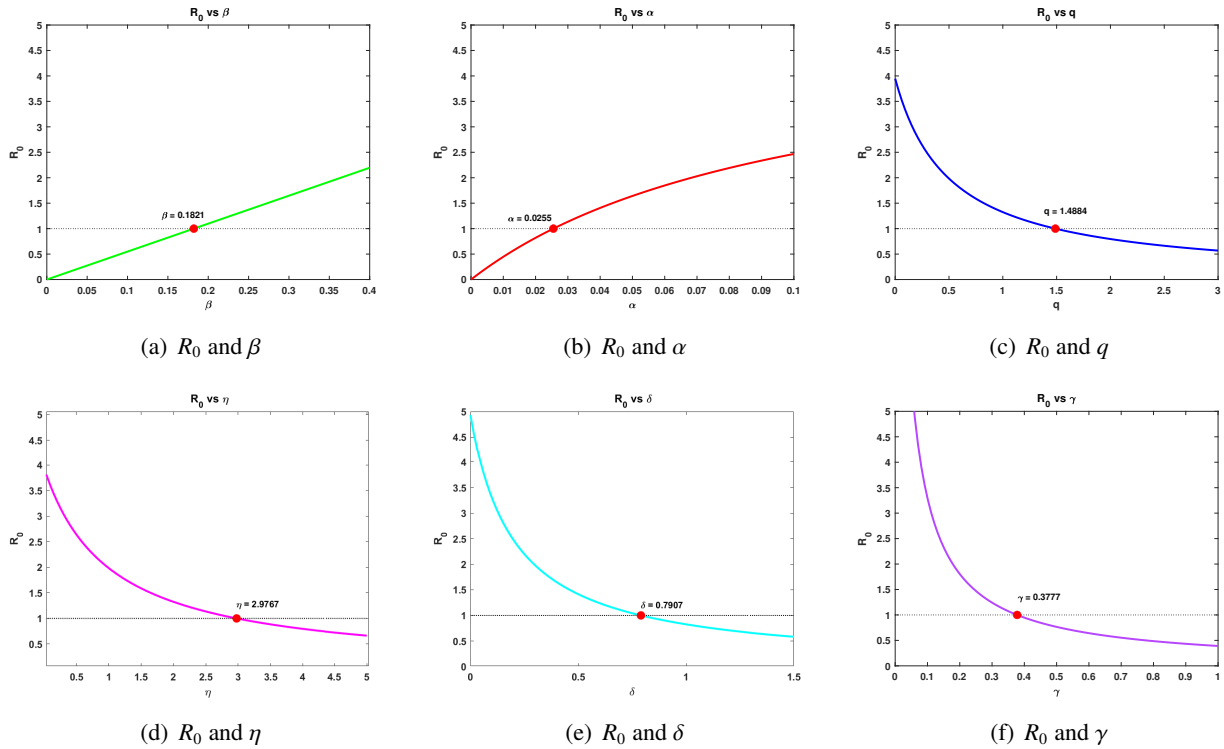

(a) R_0 and β (b) R_0 and α (c) R_0 and q

(d) R_0 and η (e) R_0 and δ (f) R_0 and γ

Figure 5. Critical parameter values at which the transcritical bifurcation occurs.

7.2. PRCC analysis

In this subsection, a global sensitivity analysis is conducted by combining Latin Hypercube Sampling (LHS) with the Partial Rank Correlation Coefficient (PRCC) method. In this procedure, model parameters are sampled across their plausible ranges for each LHS iteration, and the corresponding outcomes of the response variables H, S, E, and R_0 are recorded. The PRCC values are then computed to measure the monotonic relationships between individual parameters and each response variable, while accounting for the influence of other parameters. A total of 1000 LHS simulations are performed, and the statistical significance of the results is indicated by asterisks on the bar plots. The minimum and maximum bounds of these distributions are listed in Table 3. Figure 6 shows the PRCC values for honest taxpayers (H), susceptible (S), and evaders (E).

Table 3. Parameter ranges used in Latin Hypercube Sampling.

Parameter	β	α	γ	q	η	δ
Min	0.40	0.10	0.05	0.05	0.10	0.05
Max	0.80	0.30	0.15	0.15	0.30	0.15

(a) Honest Taxpayers (H): The PRCC results reveal that the influence of tax evader through interactions (β) and the rate at which susceptible become the tax evaders (α) are both strongly negatively correlated with the class of the honest taxpayers. In contrast, the natural reformation of evaders into honest taxpayers (γ) and the return of susceptible to honesty without passing through evasion (δ) are strongly positively correlated with H. Furthermore, audit related factors, namely the

proportion of evaders subject to inspection (q) and the probability that an audit successfully compels tax evaders to return to honest tax payers population (η), exhibit moderate positive effects. These outcomes suggest that higher influence rate (β) or greater susceptibility to evasion (α) decreases the honest taxpayers, while enhanced reformation mechanisms (γ), effective pathways for susceptible honest taxpayers (δ), and stronger auditing measures (q, η) collectively increase the proportion of honest taxpayers.

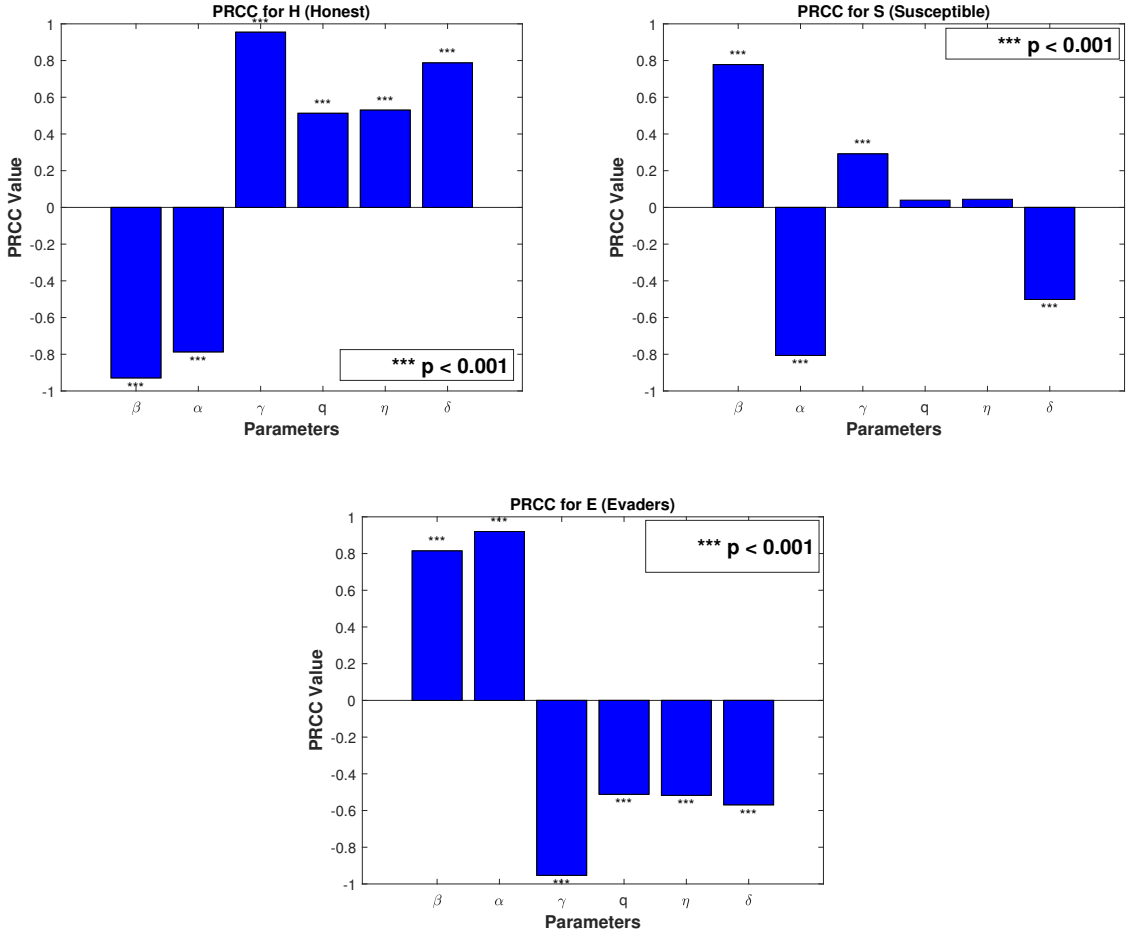

Figure 6. PRCC values for honest taxpayers (H), susceptible (S), and evaders (E).

(b) Susceptible (S): For the susceptible population, PRCC analysis shows a strong positive correlation with the influence of evaders (β), indicating that greater exposure to evaders increases dissatisfaction among susceptible taxpayers. Conversely, the transition of susceptible into tax evaders (α) and honest taxpayers (δ) are both negatively correlated with S, as these processes reduce the susceptible population. The reform of tax evaders into honest taxpayers (γ) demonstrates a small positive association with S, while audit-related parameters (q and η) exhibit negligible effects. These findings suggest that the influence of tax evaders primarily expands the susceptible class, whereas conversion dynamics and return pathways reduce the population of susceptible.

(c)Tax Evaders (E): The prevalence of tax evaders is strongly and positively correlated with the

influence rate (β) and the transition rate from susceptibles to tax evaders (α). In contrast, the natural reformation rate (γ), the transmission rate of susceptible to honest tax payers (δ), and the audit-related parameters (q and η) show strong negative correlations with E. This indicates that higher social influence and susceptibility drive evasion, while increased reformation opportunities, stronger return pathways, and effective auditing serve as mechanisms for reducing the evader class.

The basic reproduction number R_0, which reflects the potential for tax evasion to persist within the population, exhibits a positive PRCC value with the transmission parameter (β) and the susceptible-to-evader transmission rate (α). In contrast, R_0 shows a negative PRCC value with the natural reformation rate (γ), the susceptible to honest taxpayers transition rate (δ), and the audit-related parameters (q and η). These findings indicate that evasion is more likely to spread when influence rate and transmission rate are dominant, whereas stronger reformation pathways and enhanced audit policies act as effective mechanisms to reduce R_0 and limit the persistence of evasion. These results are illustrated in Figure 7.

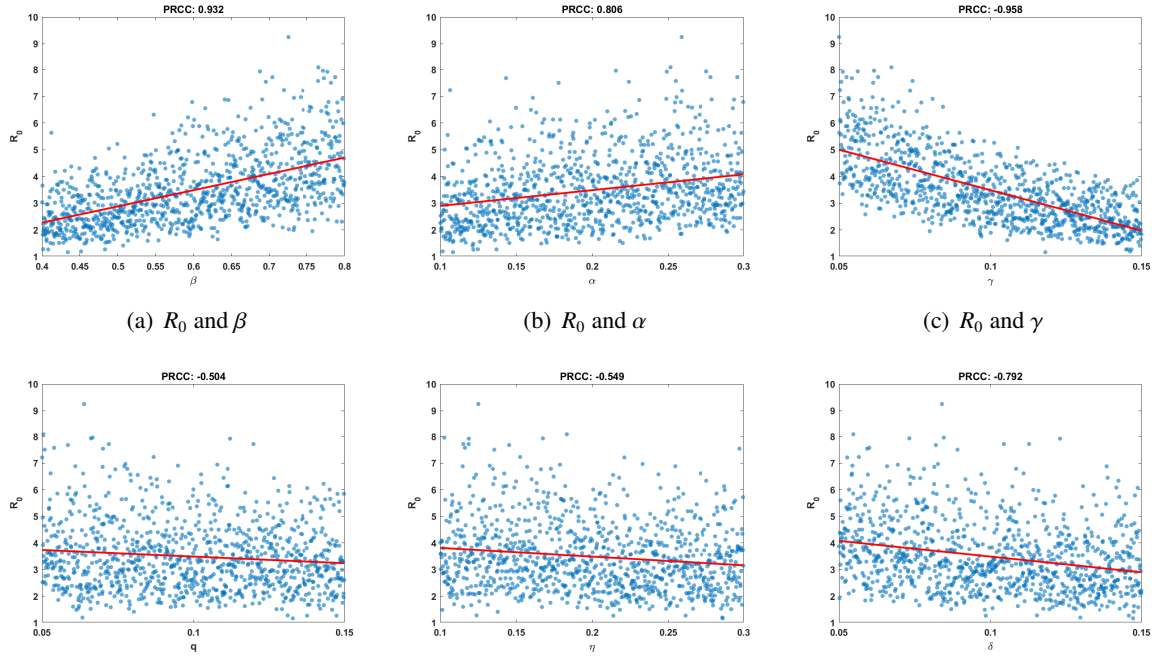

(a) R_0 and β (b) R_0 and α (c) R_0 and γ

(d) R_0 and q (e) R_0 and η (f) R_0 and δ

Figure 7. PRCC values for basic reproduction number (R_0).

8. The modified fractional Euler method

In this section, we discuss the modified fractional Euler method and its application to the governing equation (3.4) and its error estimation.

Consider the general fractional differential equation with Caputo derivative of order $0 < \rho \leq 1$:

$$^{C}D^{\rho}y(t) = f(t, y(t)), \quad y(0) = y_0, \quad t \in [0, T].$$

The interval $[0, T]$ is divided into n equal subintervals of length $h = T/n$, with nodes defined by $t_{j+1} = t_j + h$ for $j = 0, 1, \ldots, n$. Suppose that the fractional derivatives $D^{\ell\rho}y(t)$, for $\ell = 0, 1, 2$, are continuous on $[0, T]$. Expanding $y(t)$ about the initial point $t_0 = 0$ gives

$$y(t) = y(t_0) + \frac{{}^{C}D^{\rho}y(t_0)}{\Gamma(\rho+1)}\,t^{\rho} + \frac{{}^{C}D^{2\rho}y(\xi)}{\Gamma(2\rho+1)}\,t^{2\rho}, \quad 0 < \xi < T.$$

Substituting ${}^{C}D^{\rho}y(t_0) = f(t_0, y(t_0))$ and using $t_1 - t_0 = h$, one obtains

$$y(t_1) = y(t_0) + \frac{h^{\rho}}{\Gamma(\rho+1)}f(t_0, y(t_0)) + \frac{h^{2\rho}}{\Gamma(2\rho+1)}{}^{C}D^{2\rho}y(\xi).$$

If the step size h is chosen sufficiently small, the higher-order term can be neglected, giving the approximation

$$y(t_1) = y(t_0) + \frac{h^{\rho}}{\Gamma(\rho+1)}f(t_0, y(t_0)).$$

Repeating this process generates a sequence of approximations $y_j = y(t_j)$ at the nodes t_j, $j = 0, 1, 2, \ldots, n$. The resulting generalized Euler method (GEM) is expressed as

$$y(t_{j+1}) = y(t_j) + \frac{h^{\rho}}{\Gamma(\rho+1)}f(t_j, y(t_j)), \quad j = 0, 1, \ldots, n-1.$$

The modified fractional Euler method (MFEM) [20] takes the form

$$y(t_{j+1}) = y(t_j) + \frac{h^{\rho}}{\Gamma(\rho+1)}f\Big(t_j + \tfrac{h^{\rho}}{2\Gamma(\rho+1)},\ y(t_j) + \tfrac{h^{\rho}}{2\Gamma(\rho+1)}f(t_j, y(t_j))\Big), \quad j = 0 \cdot n - 1. \tag{8.1}$$

8.1. Solution for the tax evasion model

To find the approximate solutions for the fractional-order tax evasion model using the MFEM, we consider the model in compact form as:

$${}^{C}D_t^{\rho}X_r(t) = \mathbb{G}_r(H, S, E, t), \quad r = 1, 2, 3,$$

where the components are given by

$$\begin{aligned}
\mathbb{G}_1(H, S, E, t) &= \Lambda - \frac{\beta\, H(t)\, E(t)}{N} + \delta\, S(t) + \gamma\, E(t) + q\eta\, E(t) - d\, H(t),\\
\mathbb{G}_2(H, S, E, t) &= \frac{\beta\, H(t)\, E(t)}{N} - (\alpha + \delta)S(t) - d\, S(t),\\
\mathbb{G}_3(H, S, E, t) &= \alpha\, S(t) - \gamma\, E(t) - q\eta\, E(t) - d\, E(t).
\end{aligned}$$

Let us assume that $D^{k\rho}X_r(t)$, for $k = 0, 1, 2$, remain continuous on the interval $[0, T]$. Under this assumption, the numerical solutions $X_r(t_k)$, $r = 1, 2, 3$, of the system can be approximated using the MFEM iterative relation (8.1):

$$X_r(t_{j+1}) = X_r(t_j) + \frac{h^{\rho}}{\Gamma(\rho+1)}\mathbb{G}_r\left(t_j + \frac{h^{\rho}}{2\Gamma(\rho+1)},\ X_r(t_j) + \frac{h^{\rho}}{2\Gamma(\rho+1)}\mathbb{G}_r(t_j, H(t_j), S(t_j), E(t_j))\right),$$

for $r = 1, 2, 3$.

Theorem 8.1. *[20] Let f be continuous and satisfy a Lipschitz condition in y with Lipschitz constant $\mathbb{L}$ on $\omega = [a, b] \times \mathbb{R}$.*

$$|f(t, y_1) - f(t, y_2)| \leq \mathbb{L}|y_1 - y_2|. \tag{8.2}$$

Assume there exists a constant $\delta > 0$ such that

$$\left|{}^{C}D^{n\rho}y(t)\right| \leq \delta, \quad \forall\, t \in [a, b].$$

Then the numerical solution satisfies the error bound

$$|y_k - y(t_k)| \leq \eta(e^{k\theta} - 1), \quad k = 0, 1, \ldots, n, \tag{8.3}$$

where the constants are defined by

$$\eta = \frac{2\Gamma^2(\rho + 1)\, h^{2\rho}\delta}{\Gamma(2\rho + 1)(2\Gamma(\rho + 1)h^{\rho} + h^{2\rho}\mathbb{L})}, \quad \theta = \frac{2\Gamma(\rho + 1)h^{\rho} + h^{2\rho}\mathbb{L}}{2\Gamma^2(\rho + 1)}.$$

Proof. The detailed proof of this theorem is provided in [20] .

□

8.2. Numerical simulation

In this section, we present a numerical simulation of the proposed model (3.4) over the interval $[0, 100]$ for varying values of the fractional order ρ, as well as key parameters such as transmission rates, natural reformation rate, and audit-related rates. The numerical values used for the simulation are provided in Table 1. The initial condition for the present model is $H(0) = 750, S(0) = 50$ and $E(0) = 0$. The computation is done via MATLAB. To quantitatively assess the numerical convergence and stability of the proposed computational scheme, we employ the Relative Approximate Error (RAE) [21], defined for each tax-compliance compartment as follows:

$$\mathrm{RAE}_p(t_k) = \left|\frac{p(t_{k+1}) - p(t_k)}{p(t_{k+1})}\right|, \qquad p \in \{H, S, E\}.$$

The RAE for the H, S, and E for the time steps $h = 0.100$, 0.010, and 0.001 are presented graphically in Figure 8. For the three regions, as the time step increases to its largest value of $h = 0.100$, the RAE approaches its highest value and then gradually becomes smaller as the value of the time step h is reduced. The smallest value of the time step $h = 0.001$ gives the smallest RAE for the duration of the simulation. These results show that the smaller time steps lead to a higher level of numerical accuracy, validating the expected convergence of the proposed method.

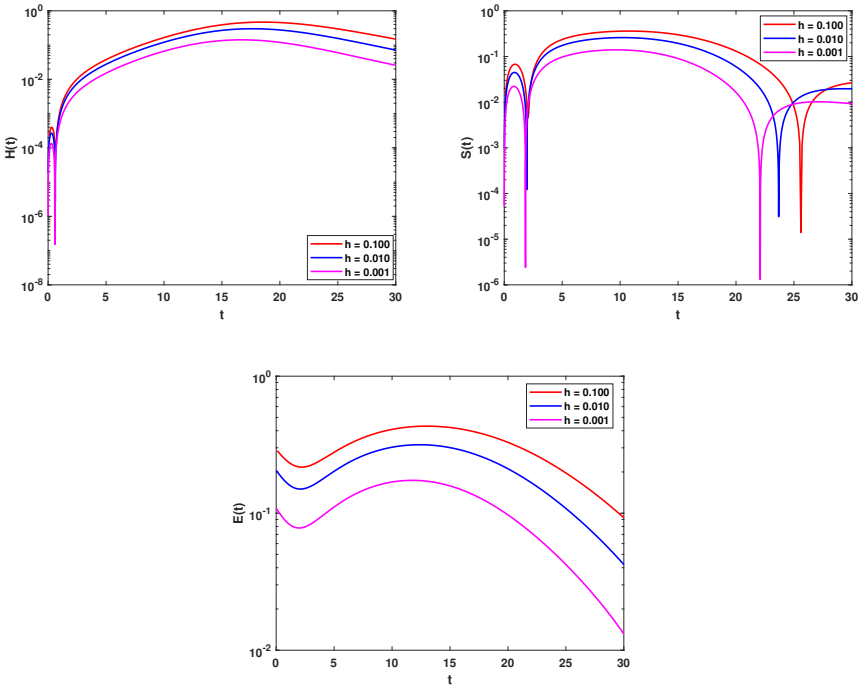

Figure 8. RAE of the compartments for varying time steps $h = 0.100, 0.010$, and 0.001.

Table 4 presents a comparative analysis of a tax evasion model using the Modified Fractional Euler Method (MFEM) and the Fractional RK4 method for fractional order $\rho = 0.90$ over $t \in [0, 100]$. The analysis demonstrates MFEM's superior accuracy and reliability in modeling tax evasion behavior patterns. The minimal absolute errors reported in Table 4 confirm the effectiveness of the proposed method.

Table 4. Comparison between modified fractional Euler and fractional RK4 methods for $\rho = 0.90$.

Compartments	Time	MFEM	Fractional RK4	Absolute Error
H	10	619.188854	619.181166	7.68×10^{-3}
	20	352.193055	352.186466	6.59×10^{-3}
	30	248.614054	248.611554	2.49×10^{-3}
	40	231.614034	231.613448	5.86×10^{-4}
	50	227.282164	227.282056	1.08×10^{-4}
S	10	92.832467	92.836423	3.95×10^{-3}
	20	196.870305	196.873194	2.88×10^{-3}
	30	205.781900	205.781932	3.20×10^{-5}
	40	201.115543	201.115416	1.27×10^{-4}
	50	198.424558	198.424531	2.70×10^{-5}
E	10	78.875577	78.879309	3.73×10^{-3}
	20	232.848817	232.852518	3.70×10^{-3}
	30	318.648344	318.650811	2.46×10^{-3}
	40	331.562162	331.562875	7.13×10^{-4}
	50	329.946281	329.946416	1.35×10^{-4}

Numerical results for different fractional orders across the time points are presented in Table 5. It is consistently observed that, as the fractional order increases from 0.80 to 0.95, the population of honest

taxpayers rises, while the population of susceptibles and tax evaders decreases. This overall trend indicates that lower fractional orders favor the growth of evaders at the expense of honest taxpayers, whereas higher fractional orders help maintain a larger proportion of honest taxpayers in the system.

Table 5. Comparison of the modified fractional Euler method for different fractional orders.

t	ρ	H	S	E
15	0.95	534.513981	132.051324	121.514269
	0.90	479.741916	155.030853	151.617068
	0.85	420.385188	176.995536	187.108976
	0.80	362.681953	194.291262	225.385518
30	0.95	268.875849	207.524130	299.962165
	0.90	248.614054	205.781900	318.648344
	0.85	237.845850	203.420074	328.057145
	0.80	232.342299	201.451731	331.368027
45	0.95	232.064431	201.326514	331.453306
	0.90	229.021852	199.667095	331.269290
	0.85	226.874745	198.104875	329.512875
	0.80	224.907332	196.469728	327.021710
60	0.95	226.545596	197.840540	329.136362
	0.90	224.514966	196.133041	326.478602
	0.85	222.350294	194.253706	323.386529
	0.80	219.966399	192.170344	319.921204
75	0.95	223.075162	194.885515	324.432870
	0.90	220.712915	192.823200	321.008353
	0.85	218.091480	190.530098	317.188314
	0.80	215.187084	187.988817	312.953041
90	0.95	219.785158	192.011814	319.657140
	0.90	217.010526	189.584309	315.612127
	0.85	213.931436	186.890127	311.121902
	0.80	210.528813	183.912826	306.159739

8.3. Effect of fractional order and key parameters

Figures 9 through 15 illustrate the numerical results of the model obtained using the proposed method.

Figure 9 presents the dynamics of all model compartments under different fractional-order values (ρ). It is understood from the figure that as the fractional order (ρ) increases, the population of honest taxpayers (H) increases, and the susceptible (S) and evader (E) populations decrease initially and gradually rise over time. This behavior occurs because the influence of fractional dynamics delays the immediate transfer of individuals from the honest taxpayer population into the other two populations. However, as time progresses, the effect of accumulation becomes more pronounced, leading to a gradual increase.

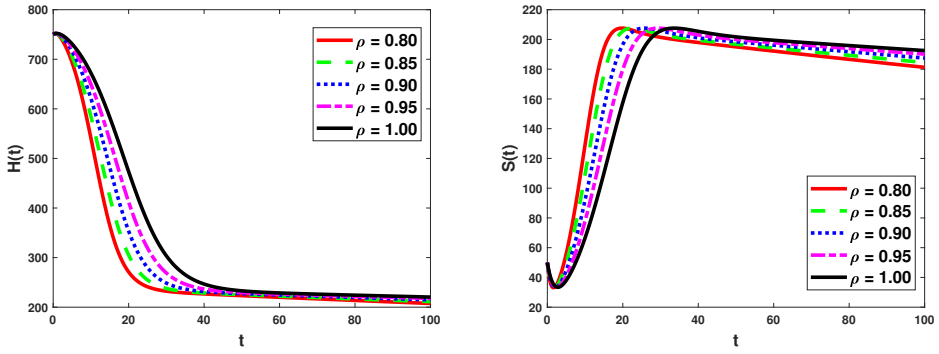

(b) S

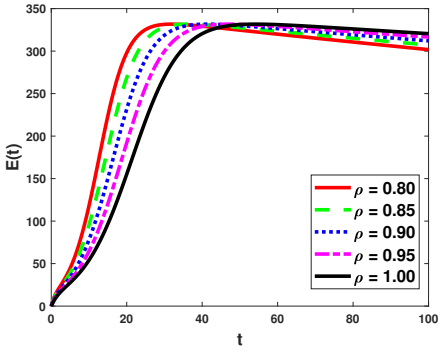

(c) E

Figure 9. Dynamics of all model compartments under varying fractional order (ρ).

Figure 10 illustrates the effect of audit success probability (η) on the populations of honest taxpayers (H) and evaders (E) for $\rho = 0.90$. An increase in η from 0.1 to 0.4 leads to a decrease in the basic reproduction number (R_0) from 3.59 to 2.83, indicating a reduction in the persistence of tax evasion. As η rises, the number of honest taxpayers increases because more evaders are successfully detected and reformed. In contrast, the number of evaders decreases significantly as η increases, demonstrating that higher audit success strongly suppresses tax evasion and promotes compliance.

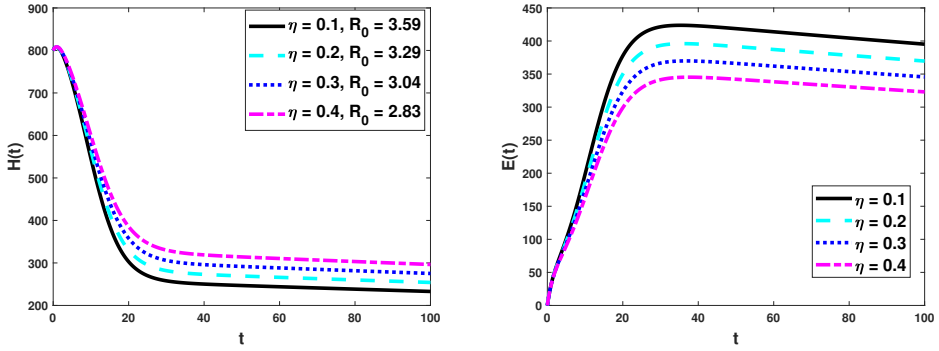

Figure 10. Effect of audit success rate (η) on the model for ρ =0.90.

Figure 11 illustrates the temporal dynamics of the honest (H), susceptible (S), and evader (E) populations under different values of the influence rate (β) for $\rho = 0.90$. A rise in β will result in a decrease in the honest class, as the influence, which speeds up the process from honest taxpayer population to other population, will result in the reduction of the honest class. Consequently, the susceptible population increases as more people become susceptible due to the influence of tax evaders. The increased susceptibility leads to a larger rise in the evader class, as evident from the rise in the value of R_0.

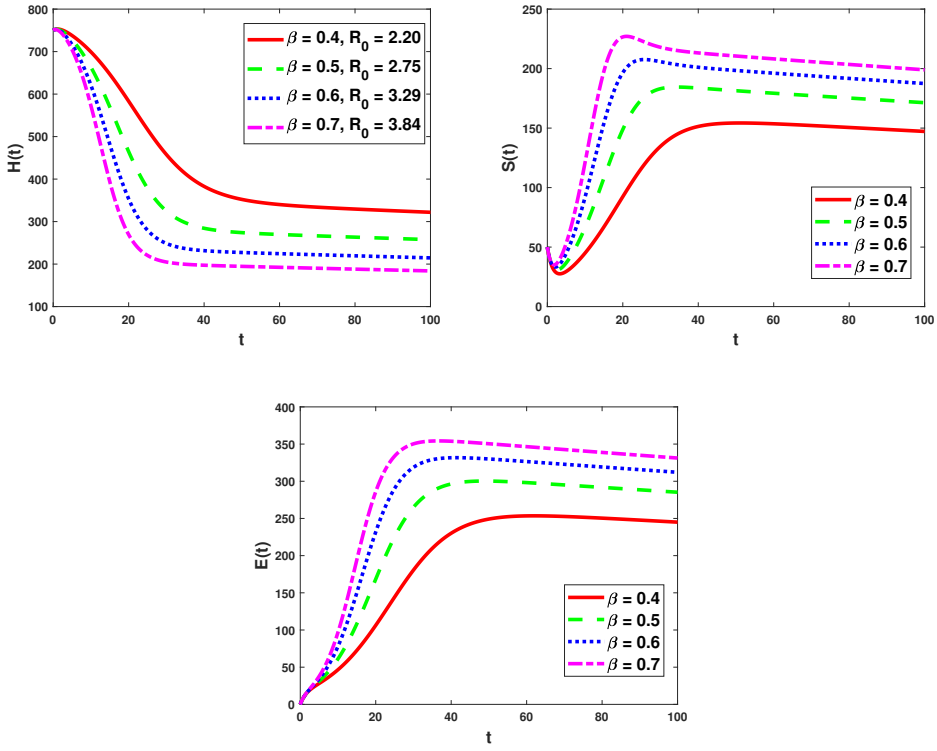

Figure 11. Dynamics of taxpayer under social influence (β) for ρ =0.90.

Figure 12 illustrates the effect of the transmission rate from susceptibles to evaders (α) in the model for $\rho = 0.90$. The figure shows that higher transmission rate (α) lead to a faster reduction in the honest taxpayers, as more individuals move toward evasion. For the susceptible class, the population initially increases but eventually decreases, since susceptibles are more quickly converted into evaders. In the scenario of evaders, the tax evaders increase more rapidly and settle at a higher level, indicating that stronger susceptibility greatly promotes tax evasion and reduces honesty, which is reflected in the corresponding increase in R_0.

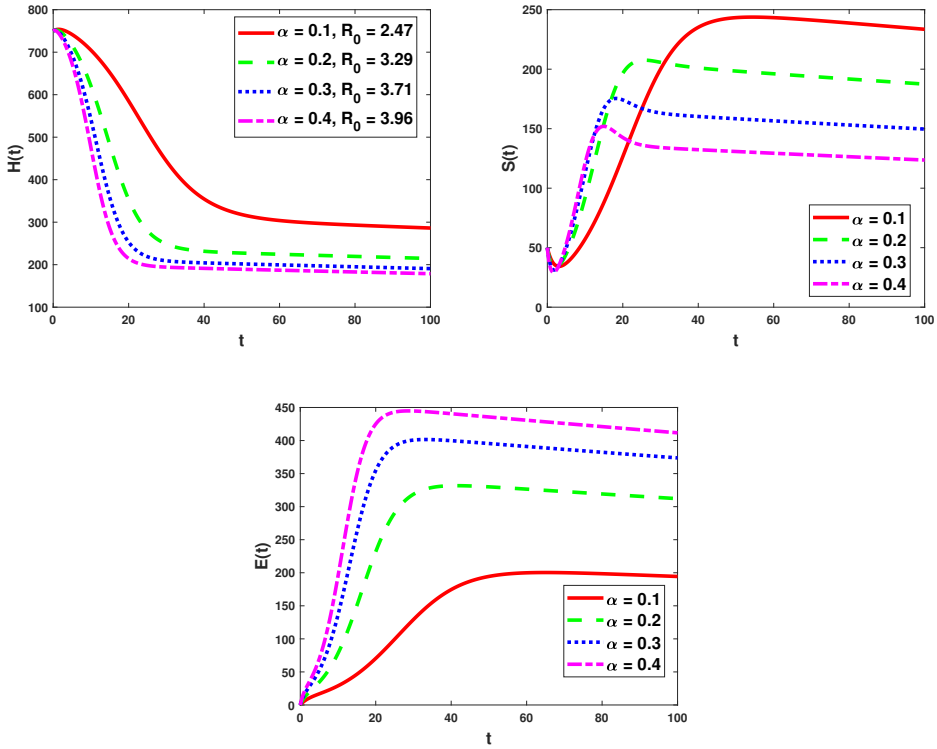

Figure 12. Effect of transmission rate (α) on the model for ρ =0.90.

Figure 13 illustrates the effect of audit rate (q) on honest tax payers (H) and evader (E) for ρ = 0.90. Here, q represents the proportion of evaders who are subject to audits. As q increases, a larger proportion of tax evaders faces the risk of being audited, which encourages compliance and leads to a noticeable rise in the population of honest tax payers.

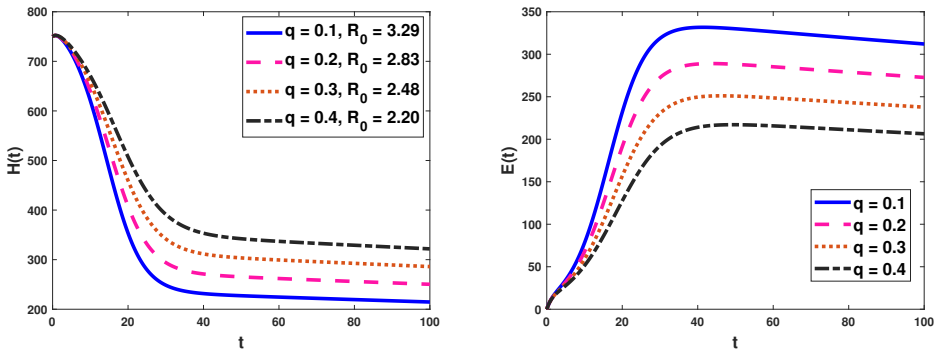

Figure 13. Effect of audit rate (q) on the model dynamics for ρ =0.90.

Figure 14 presents the effect of the susceptible to honest taxpayers transmission rate (δ) on the model dynamics for ρ = 0.90. As δ increases, the honest tax payers increases, since more susceptible return to honesty rather than shifting to tax evasion. Consequently, the susceptible and tax evader populations decrease, reflecting the reduced flow of individuals into the evading pathway. Higher

values of δ strengthen compliance by replenishing the honest class and weakening the persistence of evasion, which is also captured by the corresponding reduction in R_0.

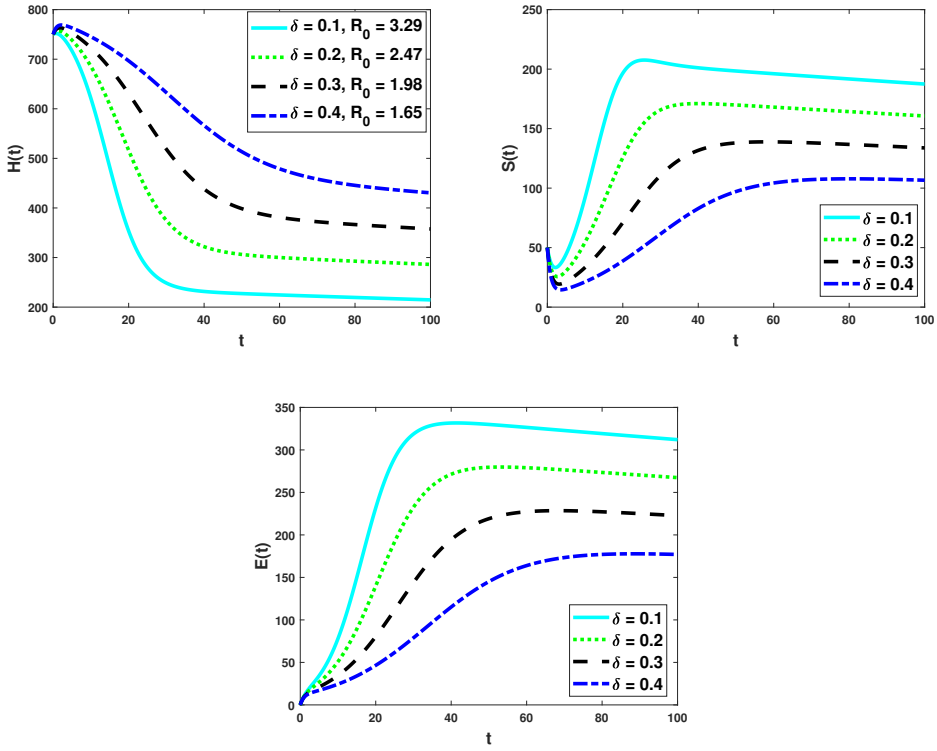

Figure 14. Effect of susceptible to honest transmission rate (δ) on population dynamics for ρ =0.90.

Figure 15 illustrates the temporal dynamics of the present model under different values of the natural reformation rate (γ) for $\rho = 0.90$. As γ increases, the honest tax payers increases, since more individuals return to honest tax payers from tax evaders. On the other hand, the susceptible population decreases, reflecting fewer taxpayers remaining dissatisfied and likely to evade. Consequently, the tax evader population shows a declining trend, as a faster transmission from evaders to the honest class limits the persistence of evasion in the system.

The evader population decreases significantly with higher audit coverage. These results emphasize the key role of audit coverage in curbing evasion, promoting honesty and lowering the basic reproduction number (R_0) of evasion behavior.

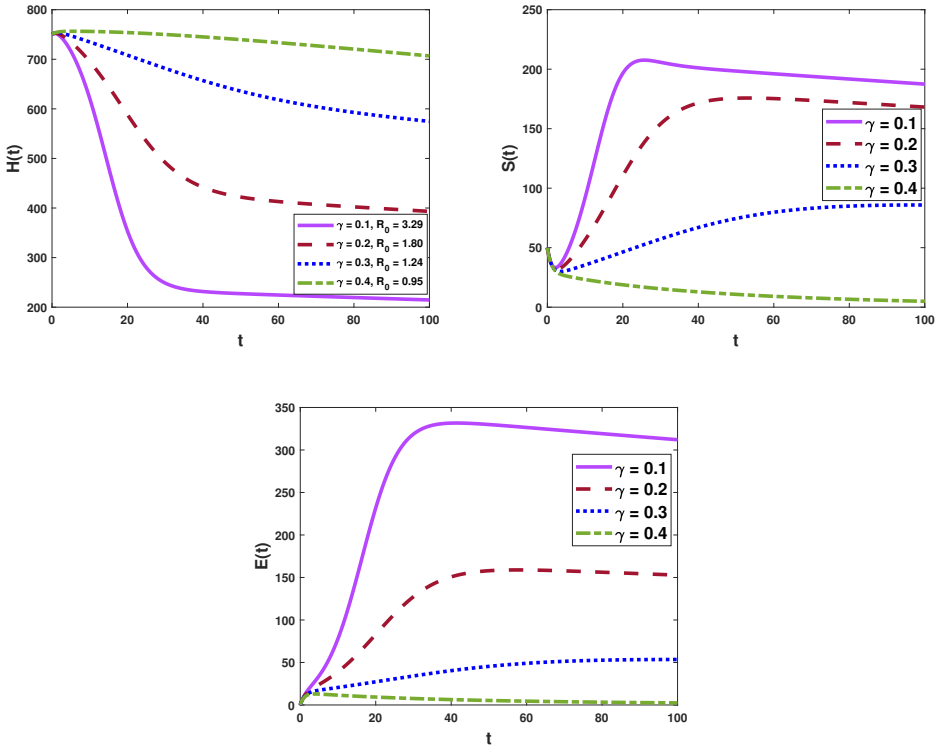

Figure 15. Effect of natural reformation rate (γ) on taxpayers for ρ =0.90.

9. Optimal control

Optimal control is an effective technique for mathematical modeling since it enables scientists to find effective solutions for reducing undesirable phenomena and optimizing effective measures. It is seen that numerical optimization in the previous section experiences the imposition of controllers on the system. To remove tax evaders, in this section, we construct a model of tax evasion, analyzing possible measures for optimizing the number of honest taxpayers and diminishing tax evaders in society. To fulfill this aim, we introduce two controls into system (3.4). The control variables in the present study are motivated by the evidence of the significance of media awareness in shaping the behavior of taxpayers [24] and the effectiveness of the government's enforcement measures, like administrative penalty, in enhancing compliance [25]. These control variables have significant relevance in the real world in the context of the measures taken by the government to discourage taxpayers from evading their responsibilities. The interpretation of each control variable of the model is as follows:

1. **Media Awareness (u_1):**

   The controller u_1 signifies the efforts of the government in raising public awareness about the need for tax compliance. In practice, this could be achieved through the use of the media, public announcements, and the dissemination of information through television, the internet, and the radio, among others. The influence of u_1 helps in the deterrence of the probability of the susceptible class moving into the evader class.

2. **Government Imposed Penalties (u_2):**

The control u_2 signifies the enforcement actions undertaken by the government to discourage people from evading taxes. These actions may take the form of tax audits, monitoring mechanisms, financial punishments, and legal actions against people caught evading taxes. These actions impose a higher cost of evasion and thus motivate people in the evader class to return to the honest taxpayers.

The system is regulated through two control functions, u_1 and u_2, defined on the finite interval $[0, t_f]$ with finite Lebesgue measure. A control value of zero corresponds to no intervention, whereas a value of one represents maximal effort. The dynamics of the system are governed by the fractional-order equations as follows:

$$\begin{aligned} {}^{C}D_t^{\rho} H(t) &= \Lambda - \frac{\beta HE(1-u_1)}{N} + \delta S + (\gamma + q\eta + u_2)E - dH, \\ {}^{C}D_t^{\rho} S(t) &= \frac{\beta HE(1-u_1)}{N} - (\alpha + \delta)S - dS, \\ {}^{C}D_t^{\rho} E(t) &= \alpha S - \gamma E - q\eta E - dE - u_2 E. \end{aligned} \tag{9.1}$$

For a fixed terminal time t_f, the objective functional is defined as

$$J(u_1, u_2) = \int_0^{t_f} \left[A_1 E + A_2 S + \frac{1}{2} B_1 u_1^2 + \frac{1}{2} B_2 u_2^2 \right] dt, \tag{9.2}$$

where $A_1, A_2, B_1, B_2 \geq 0$ are weight constants. The goal is to determine the control functions u_1 and u_2 such that

$$J(u_1, u_2) = \min_{u_1, u_2 \in \mathcal{U}} J(u_1, u_2),$$

with the control set

$$\mathcal{U} = \{u_1, u_2 \text{ are measurable}, 0 \leq u_1, u_2 \leq 1, \ t \in [0, t_f]\}. \tag{9.3}$$

The Hamiltonian for this problem is given by

$$\mathcal{H} = A_1 E + A_2 S + \frac{1}{2} B_1 u_1^2 + \frac{1}{2} B_2 u_2^2 + \lambda_H \, {}^{C}D_t^{\rho} H + \lambda_S \, {}^{C}D_t^{\rho} S + \lambda_E \, {}^{C}D_t^{\rho} E, \tag{9.4}$$

where λ_H, λ_S, and λ_E are the adjoint variables corresponding to H, S, and E, respectively. The adjoint equations corresponding to the Hamiltonian are given as follows:

$$\begin{aligned} {}^{C}D_t^{\rho} \lambda_H &= -\frac{\partial \mathcal{H}}{\partial H} = -\frac{\beta E(1-u_1)(\lambda_H - \lambda_S)}{N} + d\lambda_H, \\ {}^{C}D_t^{\rho} \lambda_S &= -\frac{\partial \mathcal{H}}{\partial S} = -A_2 + \delta(\lambda_S - \lambda_H) + \alpha(\lambda_E - \lambda_S) + d\lambda_S, \\ {}^{C}D_t^{\rho} \lambda_E &= -\frac{\partial \mathcal{H}}{\partial E} = -A_1 + (\gamma + q\eta + u_2)(\lambda_E - \lambda_H) + d\lambda_E + \frac{\beta H(1-u_1)(\lambda_H - \lambda_S)}{N}. \end{aligned}$$

Theorem 9.1. *There exist optimal controls $u_1^*, u_2^* \in \mathcal{U}$ such that $J(u_1^*, u_2^*) = \min_{u_1, u_2 \in \mathcal{U}} J(u_1, u_2)$, subject to the fractional-order system* (3.4)*.*

Proof. The controls are non-negative and bounded. For the objective functional $J(u_1, u_2) = \int_0^{t_f} \Big[A_1 E + A_2 S + \frac{1}{2} B_1 u_1^2 + \frac{1}{2} B_2 u_2^2\Big] dt$, the integrand is convex in (u_1, u_2), and the state variables (H, S, E) are bounded. Since the set of admissible controls $\mathcal{U}$ is convex, the existence of optimal controls u_1^*, u_2^* is guaranteed.

By Pontryagin's Maximum Principle, if $(H^*, S^*, E^*, u_1^*, u_2^*)$ represents the optimal solution, then there exist nontrivial adjoint functions $\lambda_H, \lambda_S,$ and λ_E, satisfying the following conditions:

$$\left.\frac{\partial \mathcal{H}}{\partial u}\right|_{u=u^*} = 0, \quad {}^{C}D_t^{\nu} \lambda = \frac{\partial \mathcal{H}}{\partial z},$$

where $\lambda = (\lambda_H, \lambda_S, \lambda_E)$ and $z = (H, S, E)$. □

Theorem 9.2. *The optimal controls u_1^*, u_2^*, which minimize J over the region $\mathcal{U}$, is given by:*

$$u_1^* = \min\{1, \max(0, \tilde{u}_1)\}, \quad u_2^* = \min\{1, \max(0, \tilde{u}_2)\},$$

where

$$\tilde{u}_1 = \frac{\beta H E(\lambda_2 - \lambda_1)}{B_1 N}, \quad \tilde{u}_2 = \frac{E(\lambda_3 - \lambda_1)}{B_2}.$$

Proof. We use the results in Pontryagin [23] and Theorem 9.1 to establish this theorem. Using the optimality condition:

$$\frac{\partial \mathcal{H}}{\partial u_1} = 0, \quad \frac{\partial \mathcal{H}}{\partial u_2} = 0,$$

we get,

$$\frac{\partial \mathcal{H}}{\partial u_1} = B_1 u_1 + \frac{\beta H E(\lambda_1 - \lambda_2)}{N} = 0, \quad \Longrightarrow u_1 = \frac{\beta H E(\lambda_2 - \lambda_1)}{B_1 N}.$$

$$\frac{\partial \mathcal{H}}{\partial u_2} = B_2 u_2 + E(\lambda_1 - \lambda_3) = 0, \quad \Longrightarrow u_2 = \frac{E(\lambda_3 - \lambda_1)}{B_2}.$$

Here, 0 is the lower bound and 1 is the upper bound for the controls u_1 and u_2. This indicates that $u_1 = u_2 = 0$, if $\tilde{u}_1 < 0$, $\tilde{u}_2 < 0$, and $u_1 = u_2 = 1$, if $\tilde{u}_1 > 1$, $\tilde{u}_2 > 1$, Hence, for these optimal controls u_1, u_2 we have found the optimum values of J.

9.1. Numerical simulation for optimal control

In this subsection, a numerical analysis of the optimal control problem (9.1) is performed using MATLAB over a simulation period of 100 days, with parameter values provided in Table 1. The weight coefficients A_1 and A_2 measure the relative importance of reducing the susceptible and evader populations, whereas B_1 and B_2 represent the economic costs associated with implementing the control strategies. To obtain the numerical solution, Euler-based numerical schemes are employed: The state equations are solved using the forward Euler method, while the adjoint equations are computed using the backward Euler method. The control strategies are studied under different scenarios as follows:

To investigate the effect of the control cost coefficients, a sensitivity analysis is conducted by varying parameters B_1 and B_2. In particular, we set $B_1 = B_2 = B$ and consider the values $B = \{10, 20, 30, 40, 50\}$. For each value of B, the optimal control problem is solved, and the resulting control profiles are obtained. The results are illustrated in Figure 16. It can be seen that lower values of B lead to stronger intervention strategies, while larger values of B reduce the magnitude of the control

functions due to higher implementation costs. Based on this analysis, $B_1 = B_2 = 10$ is used as the baseline value in the numerical simulations.

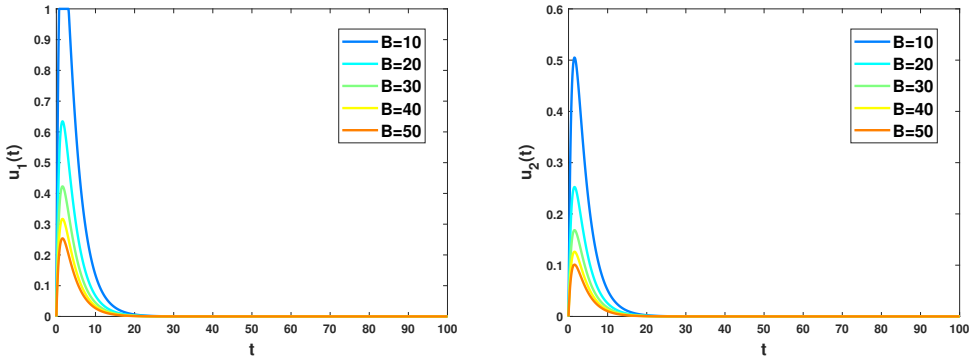

Figure 16. Optimal control profiles $u_1(t)$ and $u_2(t)$ for different values of the control cost.

9.1.1. Scenarios for intervention

The intervention analysis is carried out under two scenarios, namely Scenario I and Scenario II. These scenarios establish different conditions regarding the execution of control measures. The control variables for this purpose are u_1 and u_2, which relate to the awareness campaign through media and penalties imposed by the government, respectively. These scenario can be described as follows:

- **Scenario I (Single Control Intervention):** In this scenario, there is only one control measure tried at a time.
  - ◇ **Strategy 1:** Use of u_1 (media awareness) to make people move from the susceptible class to the honest taxpayer class.
  - ◇ **Strategy 2:** Application of u_2 (government penalties), which helps induce individuals from the evader class to switch to the honest taxpayer class.
- **Scenario II (Combined Control Intervention):** In this situation, both control methods are applied at the same time to understand the combined result.
  - ◇ **Strategy 3:** Simultaneous application of u_1 and u_2 (media awareness and government penalties).

The design of these scenarios facilitates a comparison of the efficiency of individual control measures and a combined application of these measures to assess the economic impact of interventions.

9.1.2. Scenario I

Figure 17 shows how the dynamics of the honest (H), susceptible (S), and evader (E) classes are affected by the control strategies u_1 (media awareness of the negative consequences of tax evasion) and u_2 (government-imposed penalties that encourage evaders to return to honesty). The honest class significantly decreases in the absence of any interventions ($u_1 = 0, u_2 = 0$), while the susceptible and evader classes increase, indicating the unchecked spread of evasion through social influence.

When only media awareness ($u_1 \neq 0$) is applied, individuals are better informed about the risks and consequences of evasion, which discourages susceptible from transitioning to evaders. As a result, the sizes of the susceptible and evader classes decrease, and the honest class shows noticeable growth. Similarly, evaders face stronger deterrents when only penalties ($u_2 \neq 0$) are applied, which causes them to reform into honest taxpayers and reduces the persistence of evasion.

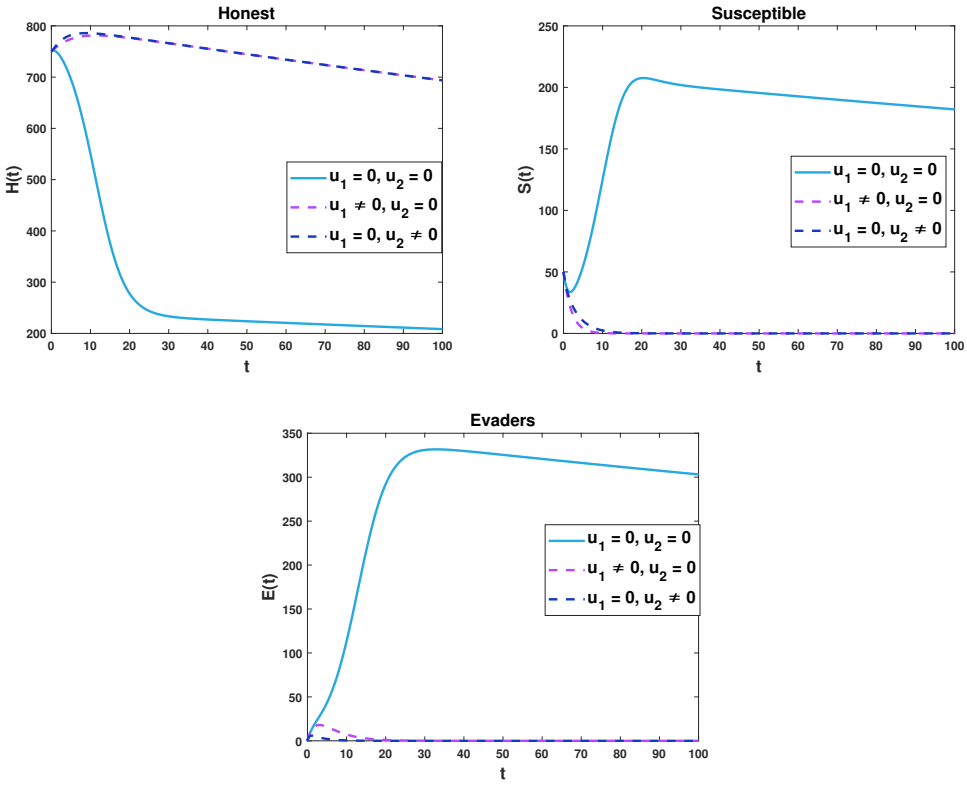

Figure 17. Effect of control measures on honest, susceptible, and evader classes.

9.1.3. Scenario II

Figure 18 presents the system dynamics under controlled and uncontrolled scenarios for integer order ($\rho = 1.0$) and fractional order ($\rho = 0.90$). Compared to the uncontrolled scenario, the implementation of control significantly raises the number of honest taxpayers in the honest class (H). This improvement results from the combined impact of government-imposed penalties and media awareness campaigns, which motivate evaders to resume compliance. Implementing control strategies efficiently lowers the number of people in the susceptible class (S) who are at risk of becoming evaders. For the evader class (E), the uncontrolled system exhibits a sharp increase in evaders, whereas the controlled system effectively suppresses this growth, keeping the evader population at minimal levels.

When comparing fractional- and integer-order systems, the fractional-order system ($\rho = 0.90$) exhibits smoother and slower transitions across all classes than the integer-order system ($\rho = 1.0$). This behavior reflects the memory effect of fractional dynamics, where past states continue to influence the current evolution. As the fractional order increases, the population of honest taxpayers grows, while the populations of susceptibles and evaders initially decreases but start to increase after some time. Overall,

the combined use of awareness campaigns and penalties ($u_1 \neq 0, u_2 \neq 0$) produces the most favorable outcome. Media awareness reduces the inflow of new evaders by lowering susceptibility, while penalties actively convert existing evaders back into the honest class. Together, these interventions significantly enhance compliance, maintain a larger honest population, and drive evasion to minimal levels.

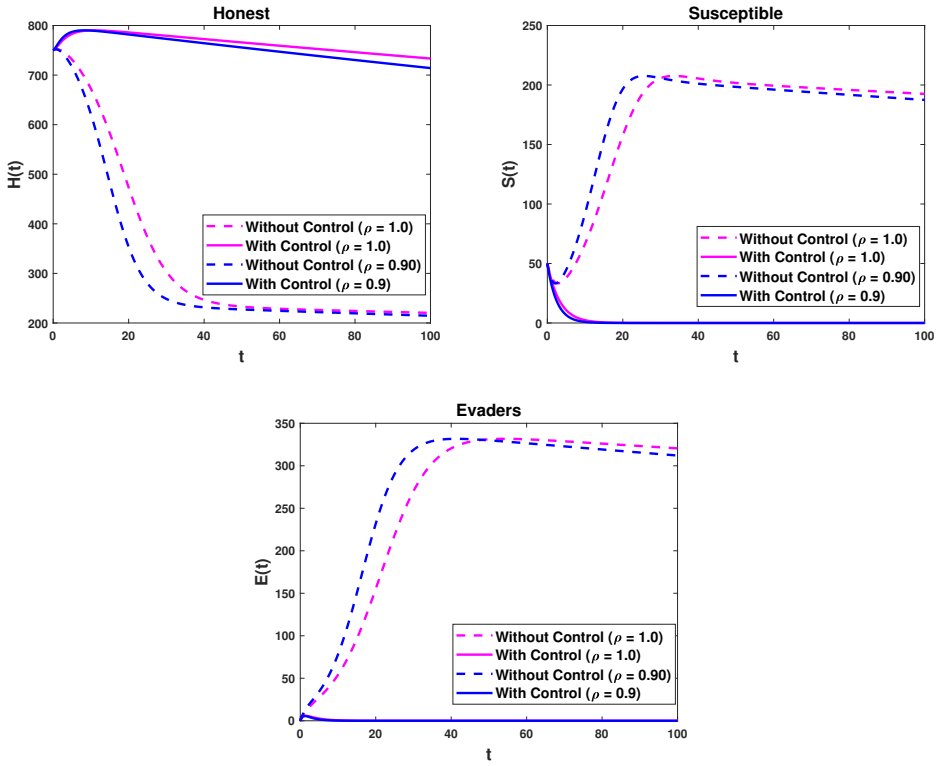

Figure 18. Role of awareness and penalties in shaping honest, susceptible, and evaders classes for $\rho = 0.9, 1.0$.

9.2. Pareto analysis for Scenario I

The Pareto analysis for the tax evasion control model is presented in Table 6 and Figure 19. The cumulative percentage is computed as follows:

$$\text{Cumulative Evaders Averted (\%)} = \left(\frac{\text{Cumulative Evaders Averted}}{\text{Total Evaders Averted}}\right) \times 100. \tag{9.5}$$

For Strategy 2:

$$\text{Strategy 2} = \left(\frac{5429}{10756}\right) \times 100 = 50.5\%. \tag{9.6}$$

Other cumulative values follow similarly. Since 80% of the total evaders averted is 8604.8, no single strategy meets this threshold individually. However, Strategy 2 represents the highest contribution.

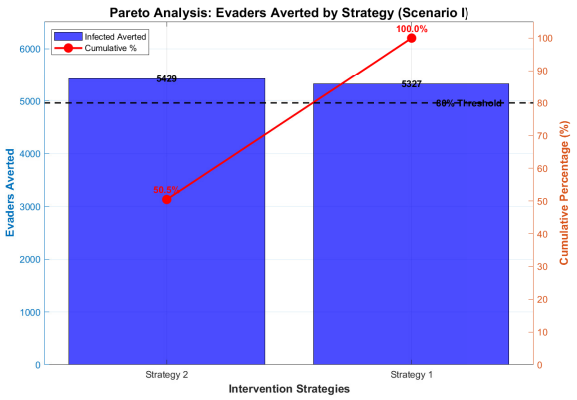

Figure 19. Pareto analysis for Scenario I.

Table 6. Pareto analysis for Scenario I.

Strategy	Evaders Averted	Cumulative	% of Total	Cumulative %
2	5429	5429	50.5%	50.5%
1	5327	10756	49.5%	100.0%

9.3. Efficiency analysis for tax evasion control strategies

The analysis shows which intervention yields the maximum reduction in tax evasion, irrespective of implementation costs. The efficiency index is calculated for each intervention strategy to determine the proportion of evaders eliminated relative to the baseline number of evaders without intervention. The Efficiency Index (E.I) is defined as:

$$\text{Efficiency Index (E.I)} = \left(\frac{\text{Total evaders averted by the intervention}}{\text{Total evaders without intervention}}\right) \times 100. \tag{9.7}$$

The efficiency outcomes reveal that all strategies are highly effective in significantly reducing tax evasion relative to the baseline of 5,449 evaders. Among the three approaches, Strategy 3 achieves the highest efficiency level of 99.76%, followed closely by Strategy 2 at 99.63% and Strategy 1 at 97.74%. Although the magnitude of difference is small, this ranking indicates that Strategy 3 provides the greatest reduction in evasion, as illustrated in Table 7 and Figure 20.

Table 7. Efficiency indices for tax evasion control strategies.

Strategy	Evaders Averted	Efficiency (%)
1	5327	97.74%
2	5429	99.63%
3	5446	99.76%

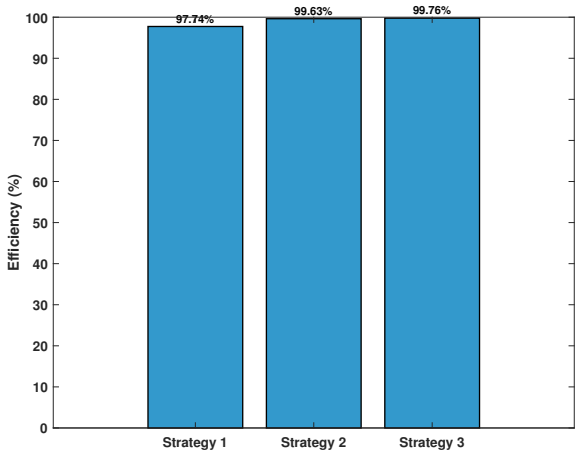

Figure 20. Efficiency indices for tax evasion strategies.

9.4. Cost-effectiveness analysis

Cost-effectiveness analysis, also referred to as economic analysis, is employed to determine the most efficient strategy and the most cost-effective intervention among the various control measures applied in the tax evasion model. This approach makes it possible to identify which intervention reduces tax evasion most effectively relative to its implementation cost. In this study, three standard measures are considered: The infection averted ratio (IAR), the average cost-effectiveness ratio (ACER), and the incremental cost-effectiveness ratio (ICER).

Definition 9.1 (**Infection Averted Ratio (IAR)**). *[26] The Infection Averted Ratio (IAR) measures the effectiveness of a control strategy by quantifying the reduction in the number of tax evaders when a particular intervention is implemented, compared with the case without intervention. It is defined as*

$$IAR = \frac{Number\ of\ evaders\ averted}{Number\ of\ individuals\ recovered\ from\ evasion}, \tag{9.8}$$

where evaders averted represents the difference between the total number of tax evaders in the absence of control and the number of evaders under the intervention strategy.

Definition 9.2 (**Average Cost-Effectiveness Ratio (ACER)**). *[26] The Average Cost-Effectiveness Ratio (ACER) gives the cost per unit reduction in tax evasion achieved by a single intervention. It is expressed as*

$$ACER = \frac{Total\ cost\ of\ implementing\ the\ control\ strategy.}{Total\ number\ of\ evasions\ prevented\ by\ the\ control\ strategy}. \tag{9.9}$$

Definition 9.3 (**Incremental Cost-Effectiveness Ratio (ICER)**). *[26] The Incremental Cost-Effectiveness Ratio (ICER) measures the change in total costs relative to the change in benefits between two competing intervention strategies. It is mathematically defined as*

$$ICER = \frac{C_2 - C_1}{E_2 - E_1}, \tag{9.10}$$

where C_1 and C_2 denote the total implementation costs of the two strategies, and E_1 and E_2 represent the corresponding numbers of tax evaders under each strategy.

Any strategy that incurs higher costs while yielding fewer benefits is considered dominated and subsequently excluded from further analysis. The final ICER values are then utilized to determine the most cost-effective option among the remaining strategies.

9.4.1. Cost-effectiveness analysis for Scenario I

Figure 21 presents a pie chart and a bar graph illustarting the IAR and ACER for Scenario I, respectively. The pie chart shows that Strategy 2 is the most effective in reducing evasion, while the bar graph indicates that Strategy 2 is the most cost-efficient. The outcomes of the IAR, ACER, and ICER calculations for Scenario I are summarized in Table 8. A comparison of Strategy 1 and Strategy 2 indicates that Strategy 2 for $\rho = 0.9$ is cost-saving relative to Strategy 1. This finding suggests that Strategy 1 is less effective and more costly than the alternatives; therefore, Strategy 1 is excluded from further consideration.

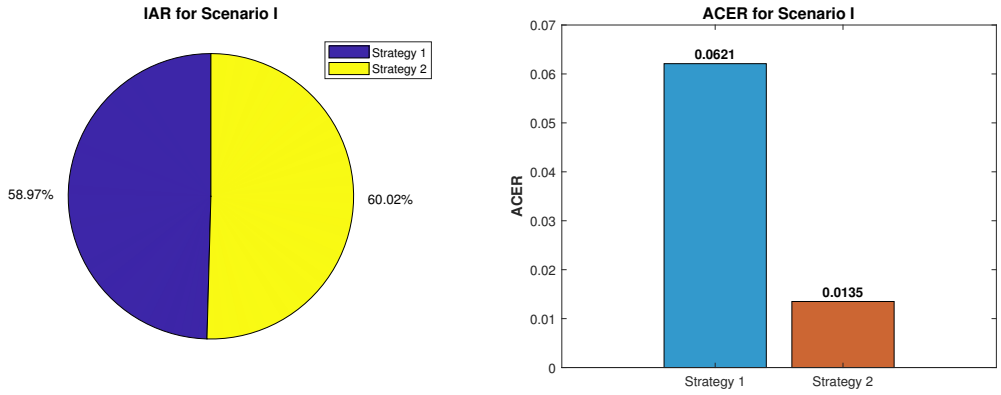

(a) IAR (b) ACER

Figure 21. (a) IAR for Scenario I and (b) ACER for Scenario I.

Table 8. Cost effectiveness analysis for Scenario I.

ρ	Strategy	Evaders Averted	Total Cost	ACER	IAR	ICER
1.0	1	5211	433.0568	0.0831	0.5701	0.0831
	2	5346	95.7962	0.0179	0.5837	-2.5089
0.9	1	5327	330.5824	0.0621	0.5897	0.0621
	2	5429	73.0697	**0.0135**	**0.6002**	**-2.5001**

9.4.2. Cost-effectiveness analysis for Scenario II

Table 9 presents the ACER and IAR for Scenario II. Strategy 3 for $\rho = 0.9$ averted the number of evaders, achieving an IAR of 0.06003 and ACER = 0.0080.

Table 9. Cost effectiveness analysis for Scenario II.

ρ	**Strategy**	**Evaders Averted**	**Total Cost**	**ACER**	**IAR**
1.0	3	5355	56.6228	0.0106	0.5840
0.9	3	5436	43.2621	**0.0080**	**0.6003**

9.4.3. Comparison of cost-effectiveness between Scenario I and Scenario II

The values of ICER for Scenario I and II are subsequently recalculated and presented in Table 10. When comparing Strategy 2 and Strategy 3, the analysis reveals that Strategy 3 is cost-saving relative to Strategy 2. This indicates that Strategy 2 is less effective and more costly, leading to its exclusion. Overall, the analysis demonstrates that Strategy 3 is the most effective intervention, as supported by its favorable ICER, IAR, and ACER values. Thus, the integration of media awareness campaigns with government-imposed penalties represents the optimal strategy for minimizing the number of evaders.

Table 10. Comparison of intervention strategies based on ICER values.

Scenario	**Strategy**	**Evaders Averted**	**Total Cost**	**ACER**	**IAR**	**ICER**
I	2	5429	73.0697	0.0135	0.6002	0.0135
II	3	5436	43.2621	**0.0080**	**0.6003**	**-4.2582**

10. Conclusions

In this study, a new fractional-order tax evasion model is proposed and analyzed using MFEM and optimal control, and the cost-effectiveness is analyzed. The model is analyzed theoretically and computationally. The findings are summarized as follows:

- The existence and uniqueness of the model are established, and local and global stability of the equilibrium points are analyzed.
- The PRCC analysis highlights the key parameters driving system dynamics. The parameters that enable evasion (α, β) are shown to greatly enhance the numbers of susceptibles and evaders, while the parameter that promotes honesty or enforcement $(\gamma, \delta, q, \eta)$ decreases it. The observations reinforce the need for intervention to reduce tax evasion.
- Numerical simulations are conducted using the Modified Fractional Euler Method, and the findings are as follows:
  - ◇ As the fractional order increases, populations of honest taxpayers, susceptibles, and evaders increase, as higher fractional order amplifies the influence of past interactions on current transmission dynamics.
  - ◇ An increase in the transmission rate decreases honest taxpayers while increasing susceptibles and evaders due to the social influence from evaders.

- ◇ A higher transmission rate from susceptibles to evaders raises the evader population while reducing honest taxpayers and susceptibles, as more individuals adopt evasion.
- ◇ An increase in the susceptible to honest transmission rate boosts honest taxpayers and reduces susceptibles and evaders, as more individuals are persuaded to comply.
- ◇ A higher natural reformation rate converts more evaders into honest taxpayers, reducing evaders and susceptibles while increasing compliance.
- ◇ Increasing the audit rate and audit success rate decreases evaders and increases honest taxpayers through effective detection.

- Pareto analysis indicates that government-imposed penalties achieve the highest reduction in evaders compared to media awareness alone.
- Efficiency analysis confirms that combining penalties with media awareness yields the greatest overall decrease in the evader population.
- Optimal control analysis is conducted using two interventions: media awareness campaigns and government-imposed penalties. The results demonstrate that both interventions individually reduce evaders, but their combined application yields the greatest reduction, effectively minimizing tax evasion in the population.
- Cost-effectiveness is evaluated using ICER, IAR, and ACER indicators, confirming that the combined strategy of media campaigns and government penalties is the most economically efficient approach, as supported by its favorable ICER, IAR, and ACER values.
- Overall, integrating media awareness campaigns with government-imposed penalties represents the optimal strategy for reducing tax evasion and promoting compliance within the population.

Author contributions

Bharathi G. S.: Writing – original draft, methodology; Sagithya Thirumalai: Writing – review & editing, visualization, supervision, methodology, conceptualization; Sekar Elango: Visualization, conceptualization; Bundit Unyong: Writing – review & editing, methodology, investigation. All authors have read and approved the final version of the manuscript for publication.

Use of Generative-AI tools declaration

The authors declare they have not used Artificial Intelligence (AI) tools in the creation of this article.

Conflict of interest

The authors have no conflict of interest to be declared here.

Data availability statement

The study does not involve any new experimental or observational data. The parameter values used in this work were obtained from previously published sources, which have been cited in the manuscript.

All results were generated through simulations based on these parameters. The datasets generated and analysed during the current study are available from the corresponding author on reasonable request.

References

1. P. T. India, Only 6.68% of population filed income tax return in 2023–24 fiscal, *Econ. Times*, December 17, 2024.
2. Taxis, *Direct tax collections for F.Y. 2025–26 as on 11.08.2025*, Government of India, August 11, 2025.
3. A. Alstadsæter, N. Johannesen, S. L. Herry, G. Zucman, Tax evasion and tax avoidance, *J. Public Econ.*, **206** (2022), 104587. https://doi.org/10.1016/j.jpubeco.2021.104587
4. N. Johannesen, P. Langetieg, D. Reck, M. Risch, J. Slemrod, Taxing hidden wealth: The consequences of US enforcement initiatives on evasive foreign accounts, *Am. Econ. J. Econ. Polic.*, **12** (2020), 312–346.
5. A. E. Biondo, G. Burgio, A. Pluchino, D. Puglisi, Taxation and evasion: A dynamic model, *J. Evol. Econ.*, **32** (2022), 797–826. https://doi.org/10.1007/s00191-022-00776-5
6. F. Menoncin, A. Modena, Dynamic tax evasion and growth with heterogeneous agents, *J. Econ. Interact. Coord.*, **20** (2025), 643–658. https://doi.org/10.1007/s11403-024-00434-y
7. F. D. Costa, A. L. Martinez, R. C. Klann, Temporal dynamics of tax avoidance: Impacts of tax audits in Brazil, *J. Int. Account. Audit. Tax.*, 2026, 100760.
8. Q. Zheng, Y. Xu, H. Liu, B. Shi, J. Wang, B. Dong, A survey of tax risk detection using data mining techniques, *Engineering*, **34** (2024), 43–59. https://doi.org/10.1016/j.eng.2023.07.014
9. M. Gombár, N. Svetozarovová, Š. Tóth, The predator-prey model of tax evasion: Foundations of a dynamic fiscal ecology, *Mathematics*, **14** (2026), 337.
10. M. Qasim, H. Ali, A. Farooq, M. Kamran, H. Ahmad, F. A. Awwad, et al., Intelligent neural framework for modeling the lifestyle-induced remission in type 2 diabetes, *Chaos Soliton. Fract.*, **205** (2026), 117841. https://doi.org/10.1016/j.chaos.2025.117841
11. J. Zhang, B. Zhou, H. Zhang, D. Yang, Fully distributed event-triggered secondary control for islanded microgrid restoration with communication link faults, *IEEE T. Autom. Sci. Eng.*, 2026.
12. R. M. Brum, N. Crokidakis, Dynamics of tax evasion through an epidemic-like model, *Int. J. Mod. Phys. C*, **28** (2017), 1750023. https://doi.org/10.1142/S0129183117500231
13. A. A. Kilbas, H. M. Srivastava, J. J. Trujillo, *Theory and applications of fractional differential equations*, Elsevier, Amsterdam, 2006.
14. I. Podlubny, *Fractional differential equations*, Academic Press, San Diego, 1999.
15. A. A. Kilbas, J. J. Trujillo, Differential equations of fractional order: Methods, results and problems—Part I, *Appl. Anal.*, **78** (2001), 153–192. https://doi.org/10.1080/00036810108840931
16. Z. Lin, H. Wang, Modeling and application of fractional-order economic growth model with time delay, *Fractal Fract.*, **5** (2021), 74. https://doi.org/10.3390/fractalfract5030074

17. M. D. Johansyah, A. K. Supriatna, E. Rusyaman, J. Saputra, Application of fractional differential equation in economic growth model: A systematic review approach, *AIMS Math.*, **6** (2021), 10266–10280. https://doi.org/10.3934/math.2021594
18. J. Sylvia, S. Ghosh, Analysis of tax evasion dynamics using the Genocchi wavelet method, *Comput. Econ.*, 2025, 1–39. https://doi.org/10.1007/s10614-025-11034-8
19. D. Matignon, Stability results for fractional differential equations with applications to control processing, *Comput. Eng. Syst. Appl.*, 1996, 963–968.
20. I. M. Batiha, A. Bataihah, A. A. Al-Nana, S. Alshorm, I. H. Jebril, A. Zraiqat, A numerical scheme for dealing with fractional initial value problem, *Int. J. Innov. Comput. Inf. Control*, **19** (2023), 763–774.
21. M. Khader, Using modified fractional Euler formula for solving the fractional smoking model, *Eur. J. Pure Appl. Math.*, **17** (2024), 2676–2691. https://doi.org/10.29020/nybg.ejpam.v17i4.5366
22. Z. M. Odibat, N. T. Shawagfeh, Generalized Taylor's formula, *Appl. Math. Comput.*, **186** (2007), 286–293. https://doi.org/10.1016/j.amc.2006.07.102
23. L. S. Pontryagin, *Mathematical theory of optimal processes*, Routledge, London, 2018.
24. H. Qi, M. Li, The impact of media attention on corporate tax avoidance: A study based on Chinese A-share listed companies, *Financ. Res. Lett.*, **58** (2023), 104594. https://doi.org/10.1016/j.frl.2023.104594
25. J. Wang, L. Li, Z. Yang, W. Liu, Tax administrative penalties and corporate tax compliance: Evidence from China, *Asian-Pac. Econ. Lit.*, 2025. https://doi.org/10.1111/apel.70023
26. F. F. Herdicho, F. Fatmawati, C. Alfiniyah, M. A. Rois, S. Martini, D. Aldila, et al., Optimal control of dengue hemorrhagic fever model by classifying sex in West Java Province, Indonesia, *Sci. Rep.*, **15** (2025), 17127.

AIMS Press